© 2021. Published by The Company of Biologists Ltd | Development (2021) 148, dev199441. doi:10.1242/dev.199441

RESEARCH ARTICLE

Kindlin2 regulates neural crest specification via integrin-independent regulation of the FGF signaling pathway

Hui Wang[1,2,*], Chengdong Wang[1,2,*], Qi Long[1,2], Yuan Zhang[1,2], Meiling Wang[3,4], Jie Liu[3], Xufeng Qi[5], Dongqing Cai[5], Gang Lu[1,6], Jianmin Sun[7], Yong-Gang Yao[8,9,10], Wood Yee Chan[2], Wai Yee Chan[1,8,11], Yi Deng[3,12,‡] and Hui Zhao[1,8,11,‡]

ABSTRACT

The focal adhesion protein Kindlin2 is essential for integrin activation, a process that is fundamental to cell-extracellular matrix adhesion. Kindlin 2 (*Fermt2*) is widely expressed in mouse embryos, and its absence causes lethality at the peri-implantation stage due to the failure to trigger integrin activation. The function of *kindlin2* during embryogenesis has not yet been fully elucidated as a result of this early embryonic lethality. Here, we showed that *kindlin2* is essential for neural crest (NC) formation in *Xenopus* embryos. Loss-of-function assays performed with *kindlin2*-specific morpholino antisense oligos (MOs) or with CRISPR/Cas9 techniques in *Xenopus* embryos severely inhibit the specification of the NC. Moreover, integrin-binding-deficient mutants of Kindlin2 rescued the phenotype caused by loss of *kindlin2*, suggesting that the function of *kindlin2* during NC specification is independent of integrins. Mechanistically, we found that Kindlin2 regulates the fibroblast growth factor (FGF) pathway, and promotes the stability of FGF receptor 1. Our study reveals a novel function of Kindlin2 in regulating the FGF signaling pathway and provides mechanistic insights into the function of Kindlin2 during NC specification.

KEY WORDS: FGF receptor, FGF signal, *Xenopus*, Kindlin2, Neural crest

[1]Key Laboratory for Regenerative Medicine, Ministry of Education, School of Biomedical Sciences, Faculty of Medicine, The Chinese University of Hong Kong, Hong Kong SAR 999077, China. [2]School of Biomedical Sciences, Faculty of Medicine, The Chinese University of Hong Kong, Hong Kong SAR, China. [3]Department of Biology, Guangdong Provincial Key Laboratory of Cell Microenvironment and Disease Research, and Shenzhen Key Laboratory of Cell Microenvironment, Southern University of Science and Technology, Shenzhen, Gunadong 518055, China. [4]School of Life Science and Technology, Harbin Institute of Technology, Harbin, Heilongjiang 150006, China. [5]Key Laboratory of Regenerative Medicine of Ministry of Education, Department of Developmental and Regenerative Biology, Jinan University, Guangzhou, Guangdong 510632, China. [6]CUHK-SDU Joint Laboratory on Reproductive Genetics, School of Biomedical Sciences, Faculty of Medicine, The Chinese University of Hong Kong, Hong Kong SAR, China. [7]Department of Pathogen Biology and Immunology, School of Basic Medical Sciences, Ningxia Medical University, 1160 Shengli Street, Yinchuan 750004, China. [8]Kunming Institute of Zoology - The Chinese University of Hong Kong (KIZ-CUHK) Joint Laboratory of Bioresources and Molecular Research of Common Diseases, Chinese Academy of Sciences, Kunming, Yunnan 650204, China. [9]Key Laboratory of Animal Models and Human Disease Mechanisms, Kunming Institute of Zoology, Chinese Academy of Sciences, Kunming, Yunnan 650223, China. [10]Kunming College of Life Science, University of Chinese Academy of Sciences, Kunming, Yunnan 650204, China. [11]Hong Kong Branch of CAS Center for Excellence in Animal Evolution and Genetics, The Chinese University of Hong Kong, New Territories, Hong Kong SAR, China. [12]Shenzhen Key Laboratory of Cell Microenvironment, Department of Chemistry, South University of Science and Technology of China, Shenzhen, Guangdong 518055, China.
*These authors contributed equally to this work

‡Authors for correspondence (zhaohui@cuhk.edu.hk; dengy@sustech.edu.cn)

Y.-G.Y., 0000-0002-2955-0693; Y.D., 0000-0003-1378-015X; H.Z., 0000-0001-8160-6415

Handling Editor: Steve Wilson
Received 21 January 2021; Accepted 14 April 2021

INTRODUCTION

Kindlin2 is an evolutionarily conserved focal adhesion protein that is involved in integrin activation and linking the extracellular matrix (ECM) and actin cytoskeleton. It contains a FERM domain, where 'FERM' represents four proteins that contain this domain: F for 4.1 protein, E for ezrin, R for radixin and M for moesin, all of which serve as membrane cytoskeleton linkers (Chishti et al., 1998). Kindlin2 binds to the cytoplasmic tail of integrin β subunits (Bledzka et al., 2012; Harburger et al., 2009; Raabe et al., 2008), which is crucial to integrin activation, and results in integrin 'inside-out' signaling that enhances the affinity of integrins for their ligands (Arnaout et al., 2005; Avraamides et al., 2008). Deletion of *Kindlin2* in mice results in early embryonic lethality, and mice carrying only one copy of the *kindlin2* (*Fermt2*) allele have aberrant angiogenesis (Montanez et al., 2008; Pluskota et al., 2011). Furthermore, embryonic stem cells isolated from *Kindlin2*-deficient mice barely adhere to the feeder layer, indicating that they have severely impaired integrin activation and cell adhesion (Bledzka et al., 2012; Montanez et al., 2008). Similar to the *kindlin2*-deficient mouse, *kindlin2* knockdown *Xenopus laevis* also show defects in vascular maintenance and angiogenic branching during embryonic development. Furthermore, depletion of maternal Kindlin2 proteins caused arrested embryonic development at early cleavage stages (Rozario et al., 2014). Intriguingly, the expression pattern of *kindlin2* in *X. laevis* embryos showed a strong tissue-specific expression in the neural crest (NC) (Canning et al., 2011). However, the function of Kindlin2 in NC development remains largely unknown.

The NC comprises a transient cell population induced at the neural plate border that is unique to vertebrate embryos. NC cells are multipotent stem cells (Baggiolini et al., 2015; Lignell et al., 2017) that give rise to a large variety of cell types, and the cranial NC cells preferentially contribute to mesenchymal cell types of facial cartilage and bone (Simoes-Costa and Bronner, 2016; Simões-Costa and Bronner, 2015; Soldatov et al., 2019). NC development can be broadly divided into formation, migration and differentiation, all of which are governed by a hierarchically arranged gene-regulatory network (Simões-Costa and Bronner, 2015). At the top of the hierarchy are signaling pathways, including the wingless-related integration site (Wnt), bone morphogenetic protein (BMP) and fibroblast growth factor (FGF) pathways. The combined action of these pathways induces the expression of a set of genes known as neural plate border specifiers, which define the neural plate border territory. Medial neural plate border specifiers, cooperating with signaling pathways that remain active during the time of specification, drive the expression of NC specifier genes such as *Foxd3*, *Ets1*, *Sox9/10* and *Snail1/2* (Mayor and Theveneau, 2013; Shellard and Mayor, 2019). NC specification is followed by the activation of the epithelial-to-mesenchymal transition machinery, which enables NC cells to detach from the epithelium

Development (2021) 148, dev199441. doi:10.1242/dev.199441

and acquire migratory ability. Guided by environmental cues, the migratory NC cells express differentiation circuits and differentiate into diverse derivatives (Mayor and Theveneau, 2013; Taylor and LaBonne, 2007). Elucidating the multi-step gene-regulatory network that governs NC development is crucial to understanding the molecular mechanisms that underlie human diseases, such as Hirschsprung's disease (a congenital gut-motility disorder) and Treacher Collins syndrome (a facial dysmorphism) (Zhang et al., 2014).

In this study, we investigated the function of *kindlin2* during NC formation using *Xenopus* embryos. We found that depletion of *kindlin2* by either morpholino oligonucleotides (MOs) or the clustered regularly interspaced short palindromic repeats (CRISPR)/CRISPR-associated protein 9 (CRISPR/Cas9) technique inhibited the expression of NC specifier genes. Consistent with the observations in whole embryos, *kindlin2* MOs inhibited NC formation induced by *wnt3a* and *chordin* in the animal cap assay. Furthermore, we showed that the FGF signaling pathway was interrupted by *kindlin2* MOs in animal cap explants and that Kindlin2 can enhance the level of FGFR1 protein. In addition, integrin activation-deficient *kindlin2* mutants also increased the FGFR1 protein level and rescued the phenotypes induced by *kindlin2* MOs in *Xenopus* embryos. These findings suggest that the function of Kindlin2 during NC formation is independent of its integrin-activating ability. Collectively, our study uncovered a novel function of Kindlin2 in NC formation via regulation of the FGF signaling pathway during embryogenesis.

RESULTS

Kindlin2 is crucial for NC formation in *Xenopus*

We examined the expression pattern of *kindlin2* throughout embryogenesis in *X. laevis* embryos and found strong *kindlin2* staining in the NC at the mid-neurula stages and late-neurula stages (Fig. S1), which is consistent with the previous studies (Canning et al., 2011). In the later developmental stages, the expression of *kindlin2* became restricted to the head, cranial NC streams and somites (Fig. S1). The expression of *kindlin2* in somites reinforces the view that Kindlin2 is essential for maintaining muscle integrity, owing to its ability to activate integrins (Dowling et al., 2008; Qi et al., 2015; Rogalski et al., 2000). However, the role of *kindlin2* in NC development remains obscure.

To investigate whether Kindlin2 plays functional roles during NC formation, we sought to perform loss-of-function assays using MOs specifically targeting *kindlin2* mRNA to block protein translation. Two MOs were designed: MO1, which targeted the 5′ UTR of *kindlin2* mRNA; and MO2, which targeted the sequence flanking the start codon of *kindlin2* mRNA (Fig. 1A). The knockdown efficiency of two MOs was assessed by western blotting, with proteins extracted from late-blastula stage embryos microinjected with either the mRNA of Myc-tagged *kindlin2* (*k2-Myc*) alone or the *k2-Myc* mRNA mixed with MO1 or MO2. The results revealed that both low (500 pg/embryo) and high (1000 pg/embryo) doses of *k2-Myc* mRNA were well expressed in the embryos, but the *k2-Myc* expression was barely detectable in the presence of either MO1 or MO2 (Fig. 1B; Fig. S2A), indicating that both MOs effectively blocked the translation of *k2-Myc* mRNA. We then performed knockdown experiments with *kindlin2* MOs to investigate the effects of *kindlin2* knockdown on NC formation in *Xenopus* embryos. Following titration of the injection doses of the two MOs, MO1 (10 ng/embryo) and MO2 (20 ng/embryo) were microinjected into one dorsal blastomere of embryos at the four-cell stage, and *lacZ* mRNA was co-injected as the lineage tracer. The other dorsal blastomere was left uninjected to serve as a control. Whole-mount *in situ* hybridization revealed that the expression of three NC specifier genes *foxd3*, *sox9* and *snail2* was significantly decreased in both the MO1-and MO2-injected embryos (Fig. 1C-E). To confirm the specificity of the *kindlin2* MOs, we performed rescue experiments with *kindlin2* mRNA containing the coding sequence only (meaning that the MOs were unable to bind to it). When the *kindlin2* mRNA was co-injected with MO1, the ratio of embryos exhibiting normal and mildly affected expression of *foxd3*, *sox9* and *snail2* was increased to 44%, 57% and 48%, respectively, compared with 0%, 33% and 18%, when MO1 was injected alone (Fig. 1C-E). Similarly, co-injection of *kindlin2* mRNA with MO2 significantly increased the ratio of embryos showing normal and mildly affected expression of *foxd3*, *sox9* and *snail2* compared with injection with MO2 alone (Fig. 1C-E). Taken together, these results suggest that Kindlin2 is crucial for NC specification.

As NC development is a gradual process that originates from the neural plate border (NPB), we wondered whether the neural plate border specification is affected by MO-mediated knockdown of *kindlin2*. To test this possibility, we examined the expression of *pax3*, one of the specifiers of the NPB, in *kindlin2* morphants at early neurula (stage 13). The expression of *pax3* was decreased in the injected side compared with the uninjected side in all MO1-injected embryos and in 70% of MO2-injected embryos (Fig. 1F; Fig. S3A), suggesting that NPB specification was inhibited by loss of *kindlin2*. As MO1 also targets *X. tropicalis kindlin2* (Fig. S2B), we injected MO1 into *X. tropicalis* embryos at the two-cell stage and examined *pax3* (*xtpax3*) expression. We found that *xtpax3* expression was also consistently suppressed in the injected side in *X. tropicalis* embryos (Fig. 1F; Fig. S3A). Taken together, these results indicate that loss of *kindlin2* inhibits NPB specification.

To substantiate the effect of *kindlin2* knockdown on NC specification, we followed the effect of *kindlin2* knockdown on the development of NC-derived tissues. As cranial NC cells make a major contribution to the development of craniofacial cartilages, we next examined craniofacial morphogenesis in *kindin2* morphants. The *kindlin2* morphants that survived to early tadpole stages displayed abnormal head morphology. Alcian Blue staining demonstrated that the sizes of Meckel's, ceratohyal and ceratobranchial cartilages were clearly reduced at the injected side in the MO1 or MO2 morphants (Fig. 1G). These results are consistent with the inhibition of NC development in the early- and mid-neurula morphants shown above (Fig. 1C-F). Taken together, these data demonstrate that Kindlin2 is required in both the induction and specification processes during NC formation, which is fundamental to the normal development of NC-derived craniofacial cartilages.

Depletion of *kindlin2* expression causes defects in cardiovascular development (Rozario et al., 2014), and in line with this observation, we found that the expression of *nkx2.5*, a marker gene for heart anlage, and *dab2*, a blood-vessel marker gene (Cheong et al., 2006; Shang et al., 2020), were repressed in *X. laevis* embryos injected with MO1 (Fig. S3B,C). This finding indicates that knockdown of *kindlin2* led to defective heart and blood-vessel formation, again supporting the specificity of *kindlin2* MOs.

Disruption of *kindlin2* in *X. tropicalis* results in decreased expression of NC regulator genes

To further validate the effect of *kindlin2* deficiency on NC formation, we used the CRISPR/Cas9 technique to disrupt *kindlin2* in *X. tropicalis*. We designed three single-guide RNAs (sgRNA) that target *X. tropicalis kindlin2* (Fig. S4A; Fig. 2A). The T7 endonuclease 1 (T7E1) assay showed that all three sgRNAs

Development (2021) 148, dev199441. doi:10.1242/dev.199441

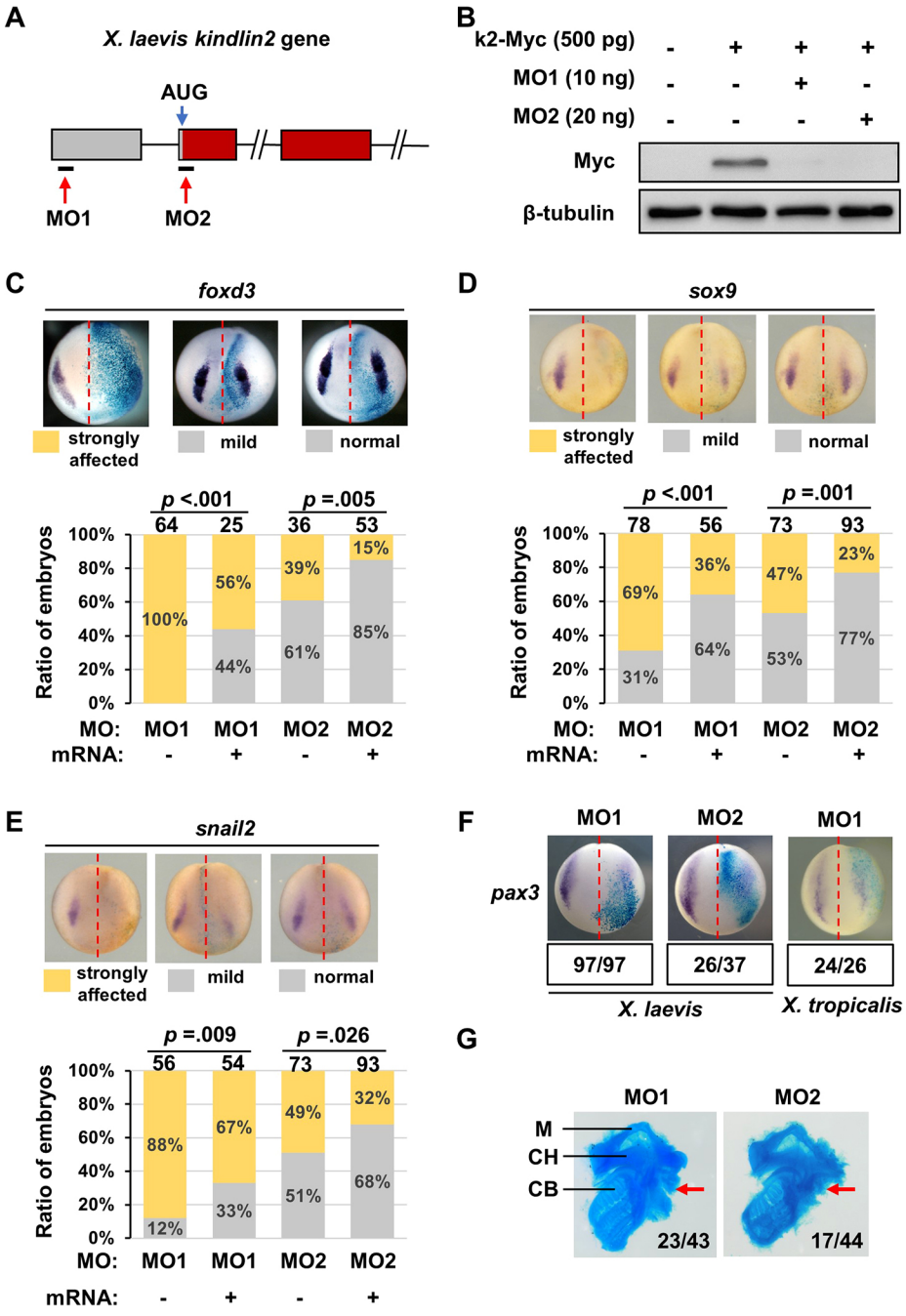

Fig. 1. Kindlin2 is required for NC formation. (A) Illustration of *kindlin2* morpholino oligonucleotide (MO)-targeting sites. (B) Kindlin2 MOs attenuate k2-Myc protein translation in embryos. Expression of k2-Myc, kindlin2 with the Myc tag at its 3′ end, was detected by western blotting using a Myc antibody, and with β-tubulin serving as the loading control. (C-E) Whole-mount *in situ* hybridization shows the expression of *foxd3*, *sox9* and *snail2* in the embryos unilaterally microinjected with MO1 alone, with a mixture of MO1 and *kindlin2* mRNA, with MO2 alone or with a mixture of MO2 and *kindlin2* mRNA. *LacZ* mRNA was co-injected to serve as a lineage tracer. Blue 5-bromo-4-chloro-3-indolyl-β-D-galactopyranoside was used as the substrate to indicate the injection side. A signal reduction of 50-100% at the injected side, relative to the uninjected side, was defined as the strongly affected phenotype; a 20-50% signal reduction was defined as the mild phenotype; and a <20% reduction was regarded as normal morphology. Representative images of classified embryos are shown in the upper panel. The numbers of mild embryos and normal embryos were counted together for bar chart and chi-squared test analysis. The total number of embryos analyzed is shown at the top of each column. (F) Expression of *pax3* in embryos of *X. laevis* or *X. tropicalis* unilaterally microinjected with *kindlin2* MOs. (G) Kindlin2 morphants that survived to tadpole stages were collected for Alcian Blue staining to examine the development of neural crest-derived craniofacial cartilages. The arrows indicate the reduction side; the numbers indicate the embryos that show the displayed pattern over the total embryos analyzed. Both MO1 (53%) and MO2 (39%) suppressed the craniofacial cartilage formation. M, Meckel's cartilage; CH, ceratohyal cartilage; CB, ceratobranchial cartilage.

could effectively disrupt *kindlin2* when co-injected with Cas9 mRNA, with sgRNA1 displaying the highest mutagenic efficacy (Fig. S4B). Moreover, when sgRNA1 and Cas9 protein were microinjected into one blastomere at the two-cell stage, the gene disruption ratio was 37% revealed by the T7E1 assay (Fig. 2B). The injected embryos were raised to neurula stage, and 17% (12/70) of them showed reduced expression of *foxd3* in the injected side (Fig. 2C). Accordingly, sgRNA1 was used to generate homozygous *kindlin2* mutant *X. tropicalis* frogs by microinjecting sgRNA1 and Cas9 mRNA into *X. tropicalis* embryos at the one-cell stage. The resulting F0 frogs were crossed with wild-type frogs to obtain heterozygous *kindlin2* mutant F1 offspring. In total, 28 (out of 60) F1 frogs carrying five different types of mutations (Fig. 2D) were obtained; five of these frogs carried frame-shift mutations, with three carrying a 10 bp deletion (hereafter referred to as k2 $\Delta10^{+/-}$), and two carrying a 2 bp deletion. The k2 $\Delta10^{+/-}$ F1 siblings were mated to obtain k2 $\Delta10^{-/-}$, i.e. homozygous *kindlin2* mutant embryos (Fig. 2E), the genotype of which was confirmed by T7E1 assay (Fig. S5A,B). Furthermore, quantitative PCR (qPCR) analysis of embryos at stage 15 (when NC is specified) showed that the level of *kindlin2* mRNA was substantially reduced in k2 $\Delta10^{-/-}$ embryos (Fig. 2F), which is likely due to nonsense-mediated mRNA decay (El-Brolosy et al., 2019; Ma et al., 2019). The mRNA level of one paralogue *kindlin1* was decreased to a lesser extent (Fig. 2F). Another paralogue *kindlin3* could not be detected by qPCR in both wild-type and k2 $\Delta10^{-/-}$ embryos at stage 15 (not shown). We next examined the expression of various NC regulators, including *foxd3*, *sox9*, *pax3*, *ets1*, *tfap2a*, *msx1*, *snail1*, *id3*, *twist1*, *sox10*, *axud1* and *c-myc*, by qPCR. It revealed that the expression of *foxd3*, *sox9*, *pax3*, *tfap2a*, *twist1*, *sox10* and *c-myc* was significantly reduced in

Development (2021) 148, dev199441. doi:10.1242/dev.199441

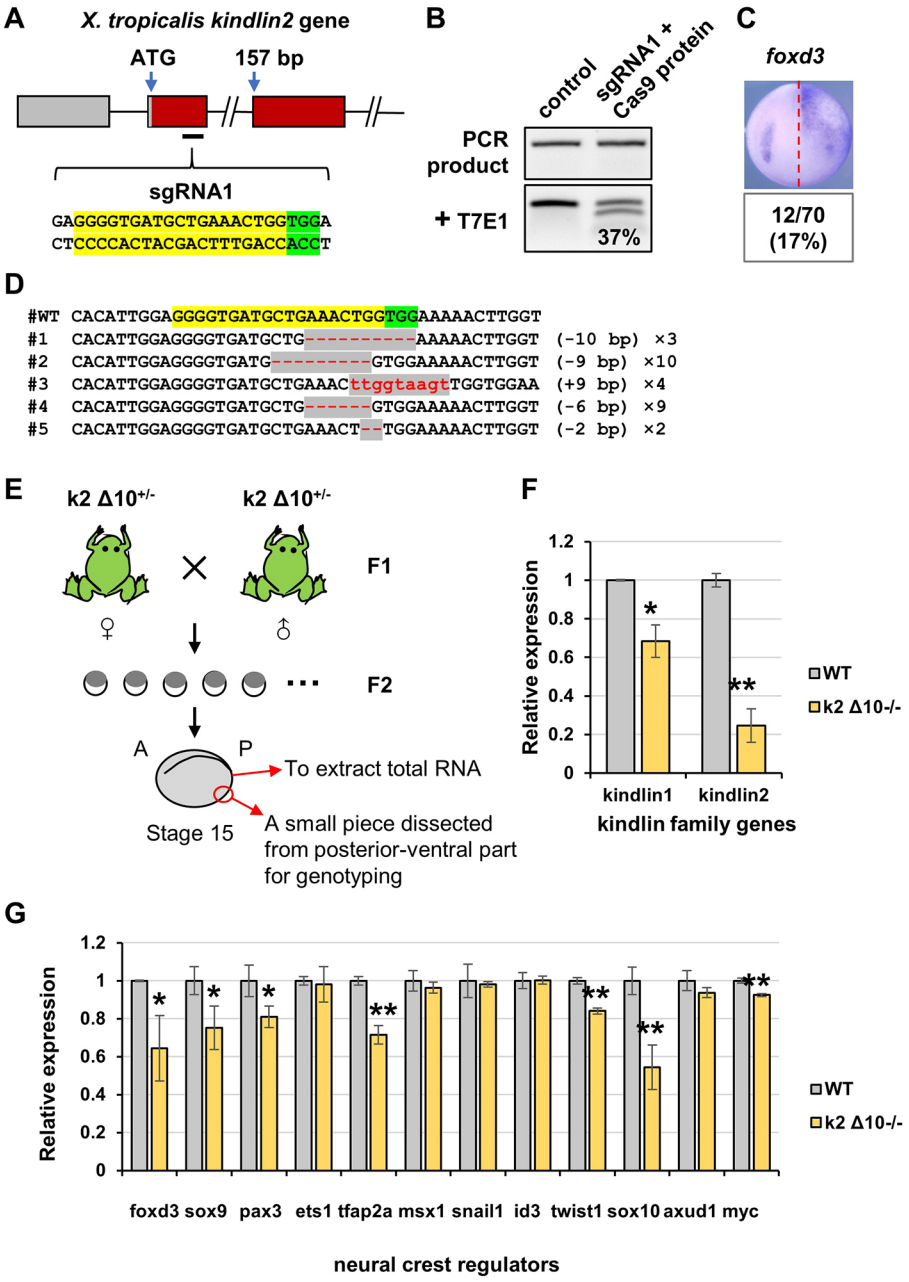

Fig. 2. CRISPR/Cas9-mediated deletion of *kindlin2* in *X. tropicalis* results in decreased expression of NC regulator genes. (A) Illustration of sgRNA1-targeting site. Gray and crimson blocks indicate the 5′-untranslated region (UTR) and coding sequence, respectively. (B) T7 endonuclease 1 enzyme assay, indicating the disruption efficiency at the *kindlin2* gene locus in embryos bilaterally microinjected with sgRNA1 and Cas9; the efficiency was calculated by ImageJ software. (C) Expression of *foxd3* in embryos unilaterally microinjected with sgRNA1 and Cas9; the embryos were from the same batch as in B. (D) Sanger sequencing results showing the F1 *X. tropicalis* frogs carrying five different mutations. (E) Schematic diagram of the examination of gene expression between k2 $\Delta10^{-/-}$ and wild-type embryos. A, anterior; P, posterior. (F,G) Gene expression determined by quantitative polymerase chain reaction in k2 $\Delta10^{-/-}$ embryos and wild-type embryos. Error bars indicate s.d. Statistical significance was analyzed using a two-tailed *t*-test (*P<0.05, **P<0.01).

k2 $\Delta10^{-/-}$ embryos compared with that in wild-type embryos (Fig. 2G), indicating that Kindlin2 is crucial for NC specification in *X. tropicalis*.

Kindlin2 deficiency inhibits NC induction and interrupts the FGF signaling pathway in animal cap explants

Having established that Kindlin2 is crucial for NC formation in *Xenopus* embryos, we next performed an *in vitro* animal cap assay to determine whether Kindlin2 deficiency affects NC induction in animal cap explants. An animal cap explant can differentiate into various tissues upon different morphogen treatment (Ariizumi et al., 2009), and Wnts mixed with BMP antagonists such as *chordin* or *noggin* can induce animal cap explants into NC-type tissues (Maharana and Schlosser, 2018; Sasai et al., 2001; Steventon et al., 2009; Wang et al., 2015; Zhao et al., 2008). We injected both blastomeres of *X. laevis* embryos at stage 2 with mixture of *wnt3a* (50 pg/embryo) and *chordin* (50 pg/embryo), dissected the animal caps at stage 9, and cultured them *in vitro* until the sibling embryos developed to stage 15, when the NC is specified (Fig. 3A). As expected, the expression of NC marker genes, including *sox10*, *snail2*, *sox9*, *foxd3*, *pax3* and *zic1*, was efficiently induced in the animal caps dissected from the embryos co-injected with *wnt3a* and *chordin*. However, the induction of these NC marker genes was significantly reduced in the animal caps co-injected with *kindlin2* MOs (Fig. 3B; Fig. S6A). This finding indicates that knockdown of *kindlin2* inhibits NC induction in animal cap explants, and provides further evidence that Kindlin2 plays a role in NC specification.

Next, we sought to investigate the underlying mechanisms of *kindlin2* knockdown on NC specification. NC formation depends on signals that arise from its surrounding tissues, including Wnt and BMP signaling in the surface ectoderm (Mayor et al., 1995; Simões-Costa and Bronner, 2015), and Wnt and FGF signaling in the underlying paraxial mesoderm (LaBonne and Bronner-Fraser, 1998; Mayor et al., 1997; Sauka-Spengler and Bronner-Fraser, 2008). As

Development (2021) 148, dev199441. doi:10.1242/dev.199441

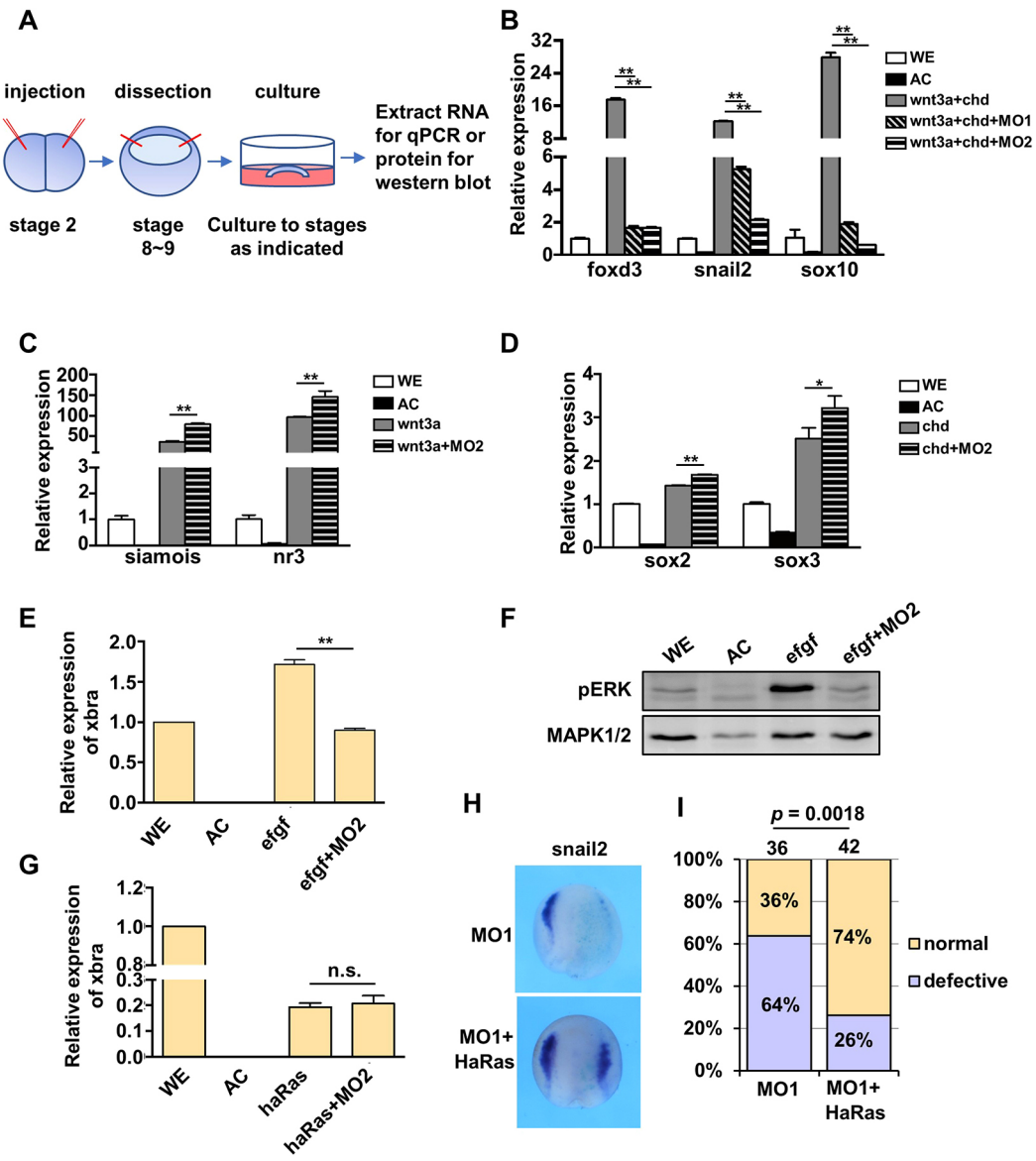

Fig. 3. Knockdown of *kindlin2* inhibits NC induction and FGF signaling pathway in an animal cap assay. (A) Schematic diagram of the animal cap assay. (B-E) Result of qPCR showing the gene expression of the NC marker genes *foxd3*, *snail2* and *sox10* (B); Wnt signaling target genes *siamois* and *nr3* (C); neural ectoderm marker genes *sox2* and *sox3* (D); and the FGF signaling target gene *xbra* (E) in animal caps injected with mRNA or a mixture of mRNA and MOs, as indicated. *Odc* (ornithine decarboxylase) served as the internal standard control. (F) Western blot showing phosphorylated extracellular signal-regulated kinase (pERK) in animal caps injected with either *efgf* or a mixture of *efgf* and MO2. Total ERK served as the loading control. (G) Result of qPCR showing the expression of *xbra* in the animal caps microinjected with *HaRas* or with *HaRas* mixed with MO2. WE, whole embryo; AC, animal cap. Data are mean±s.d. Statistical analysis was performed using an unpaired, two-tailed *t*-test. **P*<0.05, ***P*<0.01; n.s., no significant difference. (H) Expression of *snail2* in embryos unilaterally microinjected with MO1 and with MO1 mixed with *HaRas* mRNA. (I) Graph of phenotype frequency corresponding to H. The total number of embryos analyzed is shown at the top of each column. Statistical analysis was performed using a chi-squared test.

the Wnt and BMP signaling pathways are central to NC formation, we next examined both pathways in the animal caps. To examine whether knockdown of *kindlin2* affected Wnt signaling, we performed animal cap assay with the embryos injected with *wnt3a* or *wnt3a* mixed with *kindlin2* MOs. The expression of *siamois* and *nr3*, two target genes of the canonical Wnt signaling pathway, were examined by qPCR after *in vitro* culture for 3 h. The results revealed that the *wnt3a* induced expression of *siamois* and *nr3* was increased in the animal caps co-injected with *kindlin2* MOs (Fig. 3C), suggesting that knockdown of *kindlin2* does not significantly interfere with Wnt signaling activation. As suppression of BMP signaling is required for NC formation, and BMP antagonists such as Chordin are capable of transforming the epidermal cell fate of animal caps into neural cell fate, we therefore tested whether knockdown of *kindlin2* interferes with the inhibitory effects of *chordin* on BMP activity by examining the neural marker genes. To this end, the animal caps were microinjected with either chordin or chordin mixed with *kindlin2* MOs. The injected animal caps were then cultured *in vitro* until their sibling embryos developed to stage 20 when neuralization is completed. The qPCR results showed that expression of *sox2* and *sox3* was induced by *chordin*, and slightly increased by co-injection of *chordin* and *kindlin2* MO2 (Fig. 3D). These results suggest that knockdown of *kindlin2* does not alter the inhibitory effect of *chordin* on BMP signaling.

Development (2021) 148, dev199441. doi:10.1242/dev.199441

NC formation depends on signals secreted from its surrounding tissues. It is worth noting that not only was the NC suppressed in the *kindlin2* morphants, but its surrounding tissues were also disturbed, as indicated by the reduction in the expression of the paraxial mesodermal maker gene *myod* (Fig. S6B). This observation prompted us to test whether knockdown of *kindlin2* affected FGF signaling, another essential signaling pathway for NC specification (Barriga et al., 2015; Mayor et al., 1997). To this end, the animal caps were microinjected with *efgf* mRNA, which induced the expression of the FGF signaling target genes *xbra*, *egr1* and *myod*. The expression of these target genes was significantly decreased in the animal caps microinjected with *efgf* and *kindlin2* MOs (Fig. 3E; Fig. S6C). Moreover, the phosphorylation of extracellular signal-regulated kinase (ERK) induced by injection of *efgf* mRNA into animal caps was also suppressed in the presence of *kindlin2* MOs (Fig. 3F). Collectively, these results suggest that knockdown of *kindlin2* interrupts FGF signaling during NC specification.

Kindlin2 regulates the stability of the FGF receptor

The small guanine triphosphatase Ras functions as a binary molecular switch, and mediates signal transduction between the adaptor complex that binds to FGFRs and the mitogen-activated protein kinase kinase kinase (MAPKKK) (Ornitz and Itoh, 2015). To decipher how *kindlin2* might regulate the FGF signaling pathway, we examined whether *kindlin2* affects Ras signaling by microinjecting constitutively active HaRas alone or in combination with *kindlin2* MOs into animal cap explants. As expected, the expression of the FGF target gene *xbra* was efficiently induced by the constitutively active HaRas (20 pg/embryo) (Fig. 3G) (Whitman and Melton, 1992; Zhao et al., 2008). In animal caps co-injected with HaRas and *kindlin2* MOs, the expression of *xbra* remained unchanged (Fig. 3G), suggesting that FGF signaling downstream of Ras activation is unaffected by loss of *kindln2*. Moreover, HaRas rescued the NC defects in *kindlin2* morphants (Fig. 3H,I), suggesting that *kindlin2* knockdown affects NC formation occurring upstream of Ras activation in the FGF signaling cascade.

We then turned our attention to the FGFRs upstream of FGF signaling, and investigated a possible interaction between Kindlin2 and FGFR. There are four FGFRs (FGFR1-FGFR4) in *X. laevis*, and FGFR1 is crucial to the development of the NC (Brewer et al., 2016; Monsoro-Burq et al., 2003). We noticed that when FLAG-tagged *Xenopus* Kindlin2 and Myc-tagged FGFR1 were expressed in HeLa cells, a large fraction of Kindlin2-FLAG signals was found to overlap with the FGFR1-Myc signals, either on or near the cell membrane (Fig. 4A). We next examined whether Kindlin2 physically interacted with FGFR1 using a co-immunoprecipitation (co-IP) assay. Frs2, a known FGFR1-interaction partner, served as the positive control. HEK293T cells were transfected with the plasmids *kindlin2-FLAG*, *FGFR1-Myc* or *Frs2-FLAG* alone, with a combination of *kindlin2-FLAG* and *FGFR1-MYC*, or with a combination of *FGFR1-Myc* and *Frs2-FLAG*. FGFR1-Myc was co-precipitated with FRS2-FLAG, as previously reported (Fig. 4B) (Burgar et al., 2002). However, FGFR1-Myc was not detected in Kindlin2-FLAG precipitants (Fig. 4B), and FGFR1-FLAG was not detected in Kindlin2-Myc precipitants either (Fig. 4C; Fig. S7A). Thus, our data suggest that Kindlin2 interacts with FGFR1 indirectly, although they are localized closely and cannot be distinguished by standard confocal imaging. Notably, the expression of FGFR1-FLAG was enhanced in HEK293T cells co-transfected with *kindlin2-Myc* compared with that in HEK293T cells transfected with *FGFR1-FLAG* alone (Fig. 4C). We next transfected HEK293T cells with *FGFR1-FLAG* and increased doses of *kindlin2-Myc*. The plasmid pCS2-Myc was used to adjust the total amount of DNA for transfection. Western blotting showed that exogenous FGFR1-FLAG expression was increased gradually by increasing amounts of Kindlin2-Myc (Fig. 4D). Similarly, endogenous FGFR1 expression was enhanced by transfection of *kindlin2-Myc* in a dose-dependent manner (Fig. 4E). In line with this observation, the expression of phosphorylated ERK (pERK) was also increased (Fig. 4D,E), suggesting that the activity of the FGF pathway was increased. However, qPCR analysis showed that the mRNA level of *FGFR1* remained unchanged (Fig. 4F).

We next tested the effect of *kindlin2* overexpression on the FGFR1 protein level in *Xenopus* embryos. Consistent with the results obtained in HEK293T cells, overexpression of *kindlin2* in *Xenopus* embryos enhanced the protein expression of both exogenous FGFR1-FLAG and endogenous Fgfr1 in a dose-dependent manner (Fig. 4G, H). Conversely, knockdown of *kindlin2* reduced the protein expression of both exogenous FGFR1-FLAG and endogenous Fgfr1 in *Xenopus* embryos (Fig. 4I,J). Taken together, these results suggest that Kindlin2 is involved in regulating the protein level of FGFR1.

To determine whether the enhanced protein level of FGFR1 in the presence of *kindlin2* overexpression is due to increased protein stability, we measured FGFR1 protein stability following inhibition of protein synthesis by cycloheximide (CHX). Western blotting revealed that the FGFR1-FLAG protein level was markedly increased when *kindlin2-Myc* was overexpressed in HEK293T cells treated with CHX (Fig. 4K), suggesting that Kindlin2 plays a role in stabilizing FGFR1. Nedd4 and c-Cbl, two E3 ubiquitin ligases, mediate ubiquitylation of FGFR1 and promote FGFR1 degradation in lysosomes (Haugsten et al., 2008; Persaud et al., 2011; Wong et al., 2002). This led us to test whether Kindlin2 regulates FGFR1 protein stability by interacting with Nedd4 or c-Cbl. However, no interaction was detected between either Kindlin2 and Nedd4 or Kindlin-2 and c-Cbl in co-IP assays (Fig. S7B,C), suggesting that Kindlin2 is not directly involved in FGFR1 ubiquitylation. We then performed a cell-surface biotinylation assay to extract membrane-bound FGFR1 in these cells. Western blotting quantification revealed that membrane-bound FGFR1-Myc was increased in HeLa cells co-transfected with *kindlin2* compared with that in HeLa cells transfected with *FGFR1-Myc* alone (Fig. 4L). In the future, it would be interesting to examine whether Kindlin2 regulates FGFR1 endocytosis and recycling to the cell membrane.

Kindlin2 has roles in NC formation that are independent of its integrin-activating ability

As Kindlin2 is renowned for its ability to activate integrins (Rognoni et al., 2016), we next examined whether the role of Kindlin2 in NC formation is dependent on its integrin-activating ability. Analysis of the human KINDLIN2 protein structure revealed that Gln^{614} and Trp^{615} in the F3 subdomain are crucial to integrin binding, and that a mutant in which Gln^{614} and Trp^{615} were substituted by Ala (Q614A/W615A) failed to bind β1 integrin (Shi et al., 2007). Given that the kindlin2 F3 subdomain is highly conserved between human and *Xenopus*, with 96.4% sequence similarity (Fig. S8B), we introduced these Ala-substitution mutations into *Xenopus kindlin2* (hereinafter referred to as kindlin2 QW/AA). We expressed *Xenopus kindlin2* wild type or QW/AA mutant in *kindlin2* KO HT1080 cells, to assess their abilities to restore kindlin2-mediated cell shape modulation. Typically, *kindlin2* KO HT1080 cells have a shrunken morphology (cell I in Fig. 5A1) (Liu et al., 2021). However, the GFP-tagged *Xenopus kindlin2* wild type, but not the QW/AA mutant, restored

Development (2021) 148, dev199441. doi:10.1242/dev.199441

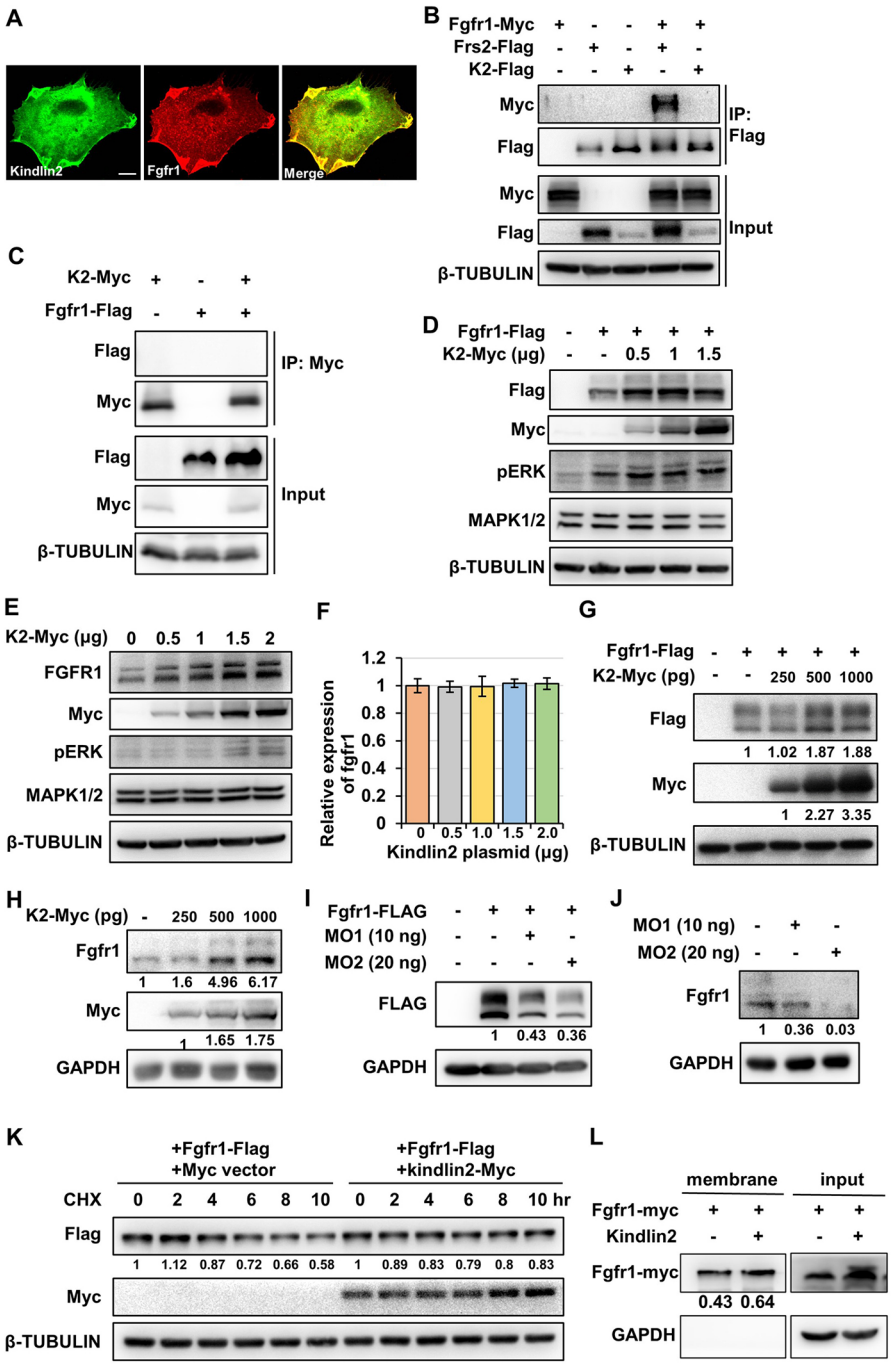

Fig. 4. Kindlin2 regulates the stability of FGFR1. (A) Colocalization of Kindlin2 and FGFR1 was analyzed by immunofluorescence staining of HeLa cells transfected with *kindlin2-FLAG* and *FGFR1-Myc* plasmid. The images were captured by confocal microscopy. Scale bar: 10 μm. (B,C) Co-immunoprecipitation assays were performed with HEK293T cells transfected with the indicated plasmids. The same amount of tagged *kindlin2* and *FGFR1* plasmids were co-transfected, and the blank vector pCS2+ was used to adjust the amount of DNA. Immunoprecipitation was performed using either a FLAG antibody (B) or Myc antibody (C). (D,E) The FGFR1 protein level was increased in the presence of Kindlin2, as revealed by western blotting. HEK293T cells were transfected with either a constant dose of *FGFR1-FLAG* plasmid (0.5 μg) and an increasing dose of *k2-Myc* plasmid (from 0 to 1.5 μg) (D), or an increasing dose of *k2-Myc* plasmid only (from 0 to 2 μg) (E). A total of 2 μg of plasmids were transfected for each group. The plasmid DNA of the pCS2-Myc vector was used to adjust the amount of DNA for transfection. (F) Results of quantitative polymerase chain reaction analysis demonstrating that *FGFR1* expression at the RNA level is not affected by the overexpression of *kindlin2*. HEK293T cells were transfected with increasing doses of *k2-Myc* plasmid (from 0 to 2 μg). Human β-actin (*ACTB*) served as the internal standard control. Data are mean±s.e.m. (G,H) The expression of FGFR1 protein was increased in *X. laevis* embryos upon overexpression of *kindlin2*. Embryos were microinjected with either a constant dose of *FGFR1-FLAG* mRNA (500 pg) and an increasing dose of *k2-Myc* mRNA, as indicated (G), or with an increasing dose of *k2-Myc* mRNA only (H). (I,J) Western blots showing the expression of exogenous (I) or endogenous (J) FGFR1 in embryos microinjected with *kindlin2* morpholino oligonucleotides. (K) Cells transfected with *FGFR1-FLAG* (2 μg) and *pCS2-Myc* vector (2 μg), or *FGFR1-FLAG* (2 μg) and *k2-Myc* (2 μg) were treated with 100 μg/ml cycloheximide 36 h after transfection, and were collected every 2 h after treatment, as indicated. The expression of FGFR1-FLAG and kindlin2-Myc was detected by western blot. (L) Membrane-localized FGFR1 was detected by western blot. β-tubulin (55 kDa) or GAPDH (36 kDa) served as the loading control. The relative expression level of FGFR1-FLAG or kindlin2-Myc to the internal standard control, as indicated in F-I,K,L, was normalized to the control after quantification using ImageJ software.

Development (2021) 148, dev199441. doi:10.1242/dev.199441

normal cell morphology (Fig. 5A-B1). Moreover, the GFP-tagged *Xenopus kindlin2* QW/AA mutant, unlike the GFP-tagged *Xenopus kindlin2* wild type, failed to localize to focal adhesions marked by paxillin (Fig. 5A-B1). We also overexpressed *Xenopus kindlin2* wild type or *kindlin2* QW/AA alone, or in combination with talin-FERM in αIIbβ3 integrin-expressing CHO A5 cells, and performed an integrin activation assay. Similar to mouse *Kindlin2* (Li et al., 2017), *Xenopus kindlin2* wild type synergized with talin for integrin activation (Fig. 5C). However, the *Xenopus kindlin2* QW/AA mutant showed significantly reduced synergistic enhancement of integrin activation (Fig. 5C). Collectively, these results indicate that the *Xenopus kindlin2* QW/AA mutant is unable to bind and activate integrins.

We next tested whether the integrin-binding-defective *kindlin2* mutant reversed the effect of *kindlin2* knockdown on NC formation in *Xenopus* embryos. To this end, we injected one dorsal blastomere of *X. laevis* embryos at the four-cell stage with *kindlin2* MO1, or *kindlin2* MO1 combined with mRNA of either *Xenopus kindlin2 QW/AA* or mRNA of the mouse *kindlin2* L675E mutant, which also fails to localize to focal adhesion and activate integrins (Li et al., 2017). Whole-mount *in situ* hybridization showed that similar to the *kindlin2* wild type (Fig. 1C,E), both *Xenopus kindlin2* QW/AA (Fig. 5D-F) and mouse *kindlin2* L675E (Fig. 5G,H) partially rescued the *kindlin2* MO-induced decreased expression of the NC marker genes *foxd3* and *snail2*. Moreover, the ratio of *kindlin2* morphants rescued by *kindlin2 QW/AA* mRNA was similar to that rescued by *kindlin2* wild-type mRNA (Fig. 1C,E). Taken together, these results suggest that the role of Kindlin2 in NC specification is independent of its integrin-activating ability. Furthermore, this function seems to be conserved across species, as the mouse integrin-binding-defective mutant reversed the *kindlin2* deficiency-induced NC defects in *Xenopus* embryos. Furthermore, overexpression of *kindlin2 QW/AA*, like that of wild-type Kindlin2 (Fig. 4G,H), enhanced the level of both exogenous and endogenous FGFR1 protein in *Xenopus* embryos (Fig. 5I,J), suggesting that the integrin-activating ability of Kindlin2 is not involved in the Kindlin2-mediated regulation of FGFR1.

Overexpression of *kindlin2* inhibits NC migration

While co-injection of wild-type *kindlin2*, *kindlin2 QW/AA* mRNA or even mouse *kindlin2 L675E* mRNA with kindlin2 MOs, reversed the *kindlin2* MO-induced downregulation of NC-specific gene expression (Fig. 1C-E; Fig. 5D-H), overexpression of any of these alone in *Xenopus* embryos had little effect on the expression of NC specifiers (Fig. 6A; Fig. S8A,C,D). These findings suggest that the overexpression of *kindlin2* does not substantially affect the NC specification process. Given that NC cells possess several integrins, including integrins α4β1 and α5β1, which mediate NC cell adhesion and migration, and convey survival signals (Bronner-Fraser, 1986; Testaz and Duband, 2001), we next investigated the effect of *kindlin2* on the early tailbud stages, when migration has already commenced. The expression of *twist*, which represses the expression of E-cadherin in delaminating NC cells and is crucial for NC migration (Simões-Costa and Bronner, 2015), was used to indicate NC migration. It revealed that microinjection of wild-type *kindlin2* mRNA, but not *kindlin2 QW/AA* mRNA, inhibited NC cell migration (Fig. 6B,C). This result suggests that a certain level of *kindlin2* is essential for the migration of NC cells, which likely occurs via an integrin-mediated mechanism.

DISCUSSION

Kindlin2 is an evolutionarily conserved protein that is essential in cell-ECM adhesion (Zhan and Zhang, 2018), and its function has been studied in both invertebrate and vertebrate model organisms. Loss of *unc112*, an ortholog of *kindlin2*, in *C. elegans* results in the most severe Pat (paralyzed, arrested elongation at twofold) phenotype (Williams and Waterston, 1994), which is due to impaired cell-ECM adhesion and integrin function (Rogalski et al., 2000). Moreover, studies in vertebrates such as mice, zebrafish and *Xenopus* have revealed that Kindlin2 is crucial to the development and function of germ layers (Montanez et al., 2008) and parts of organs, including cardiac muscle (Dowling et al., 2008; Qi et al., 2015), and angiogenesis (Pluskota et al., 2011; Rozario et al., 2014). However, *Kindlin2*-deficient mouse embryos die early (Montanez et al., 2008) and, to date, less is known about the function of Kindlin2 during vertebrate embryogenesis. In this study, we used the *Xenopus* model system to follow early embryonic development, as local loss- and gain-of-function experiments can be performed by targeted injection of *Xenopus* embryos, which are not subject to the early lethality observed in *Kindlin2*-deficient mouse embryos (Montanez et al., 2008). We demonstrated that Kindlin2 is required for NC formation and, mechanistically, we identified that Kindlin2 enhances FGFR1 stability and promotes FGF signaling, independently of Kindlin2 binding to and activating integrins. Our findings identify a novel function of Kindlin2 in NC induction and specification, and provide the first mechanistic explanation of this process.

The NC is a cell population of particular importance in embryos, as it has the potential to give rise to a wide range of cell types, such as cranial facial cartilages, peripheral neurons and melanocytes (Mayor and Theveneau, 2013). The NC originates from the neural plate border, where NC cells are induced between the neural and non-neural ectoderm during gastrulation and neurulation. Emerging evidence shows that various cellular and molecular mechanisms underlie NC formation, and highlight a level of transcriptional regulation and cell signaling interactions (Mayor and Theveneau, 2013; Shellard and Mayor, 2019). Through loss-of-function studies, we demonstrated that Kindlin2 is required for NC induction and specification in *X. laevis*. Knockdown of *kindlin2* with MOs results in inhibition of NC development, as revealed by the decreased expression of the NC-specifier genes *foxd3*, *sox9* and *snail2* in the region (Fig. 1C-E), which is rescued by *kindlin2* mRNA. Moreover, the expression of *pax3,* a specifier of the neural plate border, was also decreased in the *kindlin2* morphant, suggesting that Kindlin2 may be involved in NC induction. A previous study reported the effect of *kindlin2* knockdown with MOs in *X. laevis* (Rozario et al., 2014), but did not show the effect on NC formation that was observed in our study. We performed localized microinjection to inject one dorsal blastomere of a four-cell stage embryo with *kindlin2* MOs. This method allowed us to follow the effect on NC formation and monitor the parallel control in the same embryo, with limited effects on other tissues. In addition, we selected different target sequences of *kindlin2* MO from those used in the previous study (Rozario et al., 2014). Two MOs were designed to bind to the sequence located at the 5′-UTR of *kindlin2* and the sequence spanning the 5′-UTR (8 bp), and the beginning of the coding sequence (17 bp). Both MOs effectively and specifically knocked down *kindlin2* in *Xenopus* embryos (Fig. 1B-F; Fig. S2). Moreover, MO-mediated knockdown of *kindlin2* inhibited the NC formation induced by *wnt3a* and *chordin* in the animal cap assay (Fig. 3B; Fig. S6A).

Consistent with the inhibitory effects of *kindlin2* deficiency on NC development in early- and mid-neurula *kindlin2* morphants, the *kindlin2* morphants, which survive and develop to early tadpole stages, displayed severe facial cartilage defects (Fig. 1G). In line with the effects of *kindlin2* deficiency in *X. laevis* embryos,

Development (2021) 148, dev199441. doi:10.1242/dev.199441

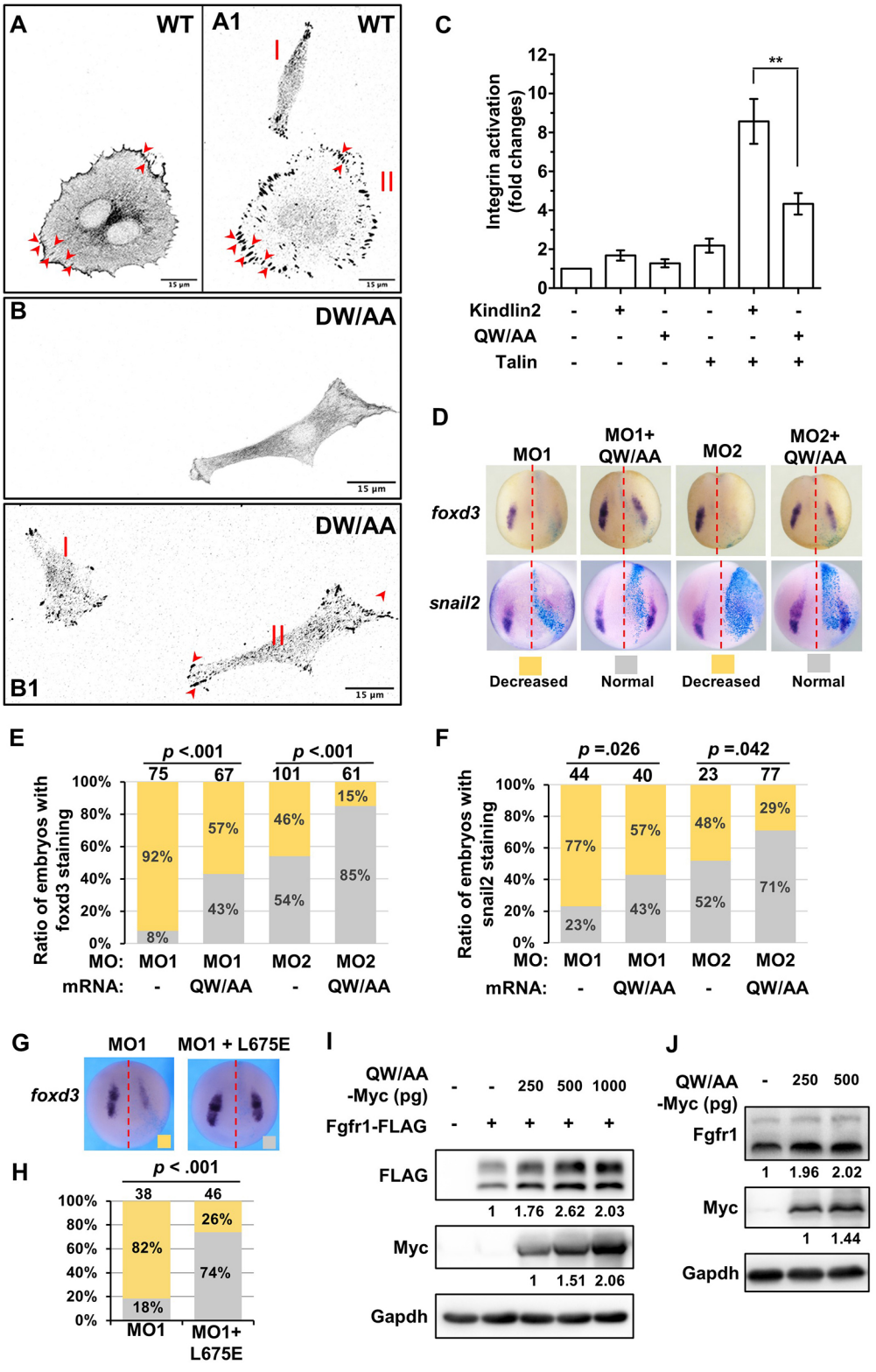

Fig. 5. The role of kindlin2 in NC formation is independent of its integrin-activating ability. (A-B1) The Kindlin2 QW/AA mutant is not localized in focal adhesion. Kindlin2 KO HT1080 cells stably expressing paxillin-mRuby2 were transfected with wild-type *Xenopus kindlin2-GPF* (A,A1) and *kindlin2-QW/AA-GFP* (B,B1). The fluorescence images were captured by confocal microscopy. Wild-type kindlin2-GFP but not kindlin2-QW/AA was localized to focal adhesion areas (arrowhead). (C) The *Xenopus* kindlin2-QW/AA showed a significant decrease in integrin-activation activity compared with that of wild-type kindlin2. Data are mean±s.d. Statistical analysis was performed using an unpaired, two-tailed *t*-test (***P*<0.01). (D) Whole-mount *in situ* hybridization showing the expression of *foxd3* and *snail2* in embryos microinjected with the indicated MOs or MOs in combination with *kindlin2 QW/AA* mRNA. (E,F) Graph of phenotype frequency for *foxd3* (E) and for *snail2* (F) that corresponds to the images shown in D. (G) Expression of *foxd3* in embryos microinjected with MOs or MOs mixed with mouse *Kindlin2 L675E* mRNA. (H) Graph of phenotype frequency corresponding to G. The total number of embryos analyzed is shown at the top of each column. A chi-squared test was used for the statistical analysis shown in E,F,H. (I,J) Western blot demonstrating the expression of FGFR1 in embryos microinjected with increasing amounts of *Kindlin2-QW/AA-Myc* mRNA (from 0 to 1000 pg/embryo) in combination with (I) or without (J) constant *FGFR1-FLAG* mRNA (500 pg). The Fgfr1 in J is endogenous Fgfr1, while I shows exogenous FGFR1. Gapdh served as the loading control. The expression of FGFR1 and Kindlin2 was quantified by ImageJ software. The signals of Kindlin2 relative to Gapdh from embryos injected with the RNA combinations were normalized to those from embryos injected with *FGFR1* mRNA alone.

depletion of *kindlin2* in *X. tropicalis* by CRISPR/Cas9 also resulted in a reduction in NC specification in F0 embryos (Fig. 2C). Furthermore, the embryos of homozygous F2 *kindlin2* deletion (k2 $\Delta10^{-/-}$) mutants at stage 15 showed significantly reduced expression of a variety of NC regulators (Fig. 2G). Collectively, these data support the notion that Kindlin2 plays an essential role in NC formation (Fig. 7A).

The animal cap assay results suggest that the effect of Kindlin2 on NC formation occurs via the FGF signaling pathway, which plays an essential role in NC formation in *Xenopus* and in the mouse. Conditional inactivation of FGFR, ERK, the upstream elements of ERK (B/C-Raf and MEK1/2) or the downstream effector serum response factor in the developing NC cells in mice results in craniofacial anomalies (Newbern et al., 2008; Wang et al., 2013). In

Development (2021) 148, dev199441. doi:10.1242/dev.199441

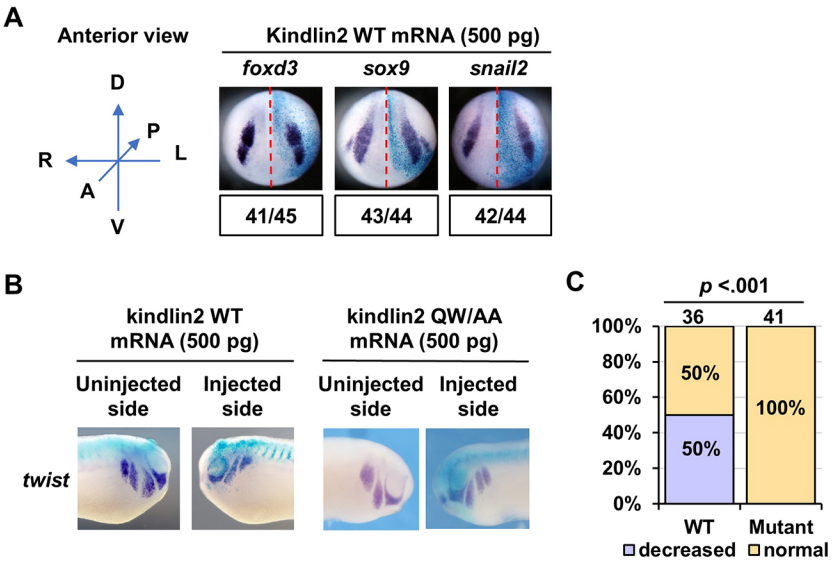

Fig. 6. Overexpression of *kindlin2* inhibits NC migration. (A) Expression of *foxd3*, *sox9* and *snail2* in embryos unilaterally microinjected with wild-type *kindlin2* mRNA (500 pg/embryo). The embryos were collected at stage 15, and the expression was examined by whole-mount *in situ* hybridization. D, dorsal; V, ventral; A, anterior; P, posterior; R, right; L, left. (B) Expression of *twist* in embryos (stage 23) unilaterally microinjected with wild-type *kindlin2* mRNA or *kindlin2 QW/AA* mRNA. (C) Graph of the phenotype frequency corresponding to B. The total number of embryos analyzed is shown at the top of each column. A chi-squared test was used for statistical analysis.

kindlin2 morphants, the NC was suppressed, and the paraxial mesoderm, which secrets FGF-signaling triggers, was also disturbed (Fig. S6B) (Sauka-Spengler and Bronner-Fraser, 2008). Furthermore, knockdown of *kindlin2* was found to attenuate the expression of FGF target genes induced by overexpression of *efgf*, such as *egr1*, *xbra* and *myod* (Fig. 3E; Fig. S6C). Concurrently, the *efgf*-induced phosphorylation of mitogen-activated protein kinase was also reduced in response to *kindlin2* knockdown (Fig. 3F). We discovered that the FGFR1 protein level was increased following overexpression of *kindlin2* in both human HEK293T cells and *Xenopus* embryos (Fig. 4D,E,G,H), and was reduced when *kindlin2* is knocked down (Fig. 4I,J). Thus, it is attractive to propose that Kindlin2 regulates FGF signaling at least in part by stabilizing FGFR1. Clearly, future studies are required to further investigate the underlying mechanisms of these processes.

Kindlin2 has key roles in integrin activation, consistent with its roles in cell-ECM adhesion (Zhan and Zhang, 2018). However, emerging evidence shows that kindlin2 has novel functions that are independent of its integrin-binding and integrin-activation abilities (Guo et al., 2015; Wei et al., 2013; Yu et al., 2013, 2012). In this

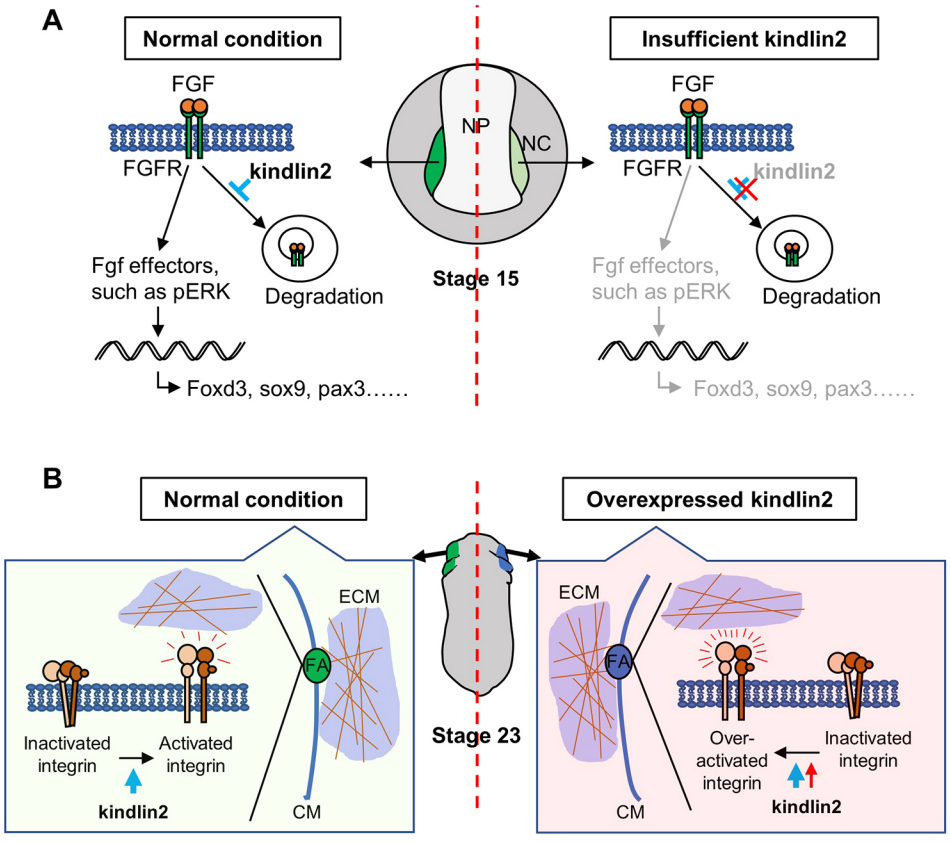

Fig. 7. Proposed working model of the effect of Kindlin2 on the development of the NC. (A) Kindlin2 is involved in mediating the stability of the FGFR during NC specification. The FGF pathway, the activity of which is maintained at a normal level, together with other signaling pathways, induces the expression of NC-specific genes. Reduction of *kindlin2* results in a decrease of FGFR protein levels, leading the FGF pathway activity to be compromised, and thus the final output. NP, neural plate. The schematic drawing is of a stage 15 embryo in anterior view, with the dorsal side positioned at the top. (B) Integrins play an essential role in the migration of NC cells. After NC specification, NC cells will delaminate through the epithelial-mesenchymal transition process and begin to migrate from the neural tube. NC cells alter their contacts with the ECM during the migration process, and these interactions are largely regulated by integrins. Integrins integrate extracellular and intracellular scaffolds at cell focal adhesion (FA) sites. Integrin activation requires kindlin2 and leads to an enhanced affinity between integrins and their ligands. However, overexpression of kindlin2 may result in the overactivation of integrins, which may interfere with the delamination and migration of NC cells. The schematic drawing is of a stage 23 embryo in dorsal view, with the head positioned at the top. CM, cell membrane; ECM, extracellular matrix; FA, focal adhesion.

Development (2021) 148, dev199441. doi:10.1242/dev.199441

study, we demonstrated that two integrin-activation-defective mutants of *kindlin2* (Q614A/W615A and L675E), like wild-type *kindlin2*, reversed the decreased expression of the NC specifier genes that were induced by *kindlin2* knockdown (Fig. 5D-H). Moreover, FGFR1 protein expression was enhanced by overexpression of *kindlin2 QW/AA* (Fig. 5I,J). However, overexpression of *kindlin2* did not substantially affect NC specification, but instead inhibited the expression of *twist*, which is involved in the regulation of NC migration (Fig. 6B,C). This effect appears to be dependent on integrin signaling, as overexpression of integrin-binding-defective mutant *kindlin2* fails to do so. As it is well established that integrins play essential roles in cell movement (De Pascalis and Etienne-Manneville, 2017; Hamidi and Ivaska, 2018), we speculate that the overexpression of *kindlin2* causes overactivation of integrins, and therefore impairs NC movement, as reflected by decreased *twist* expression (Fig. 6B,C; Fig. 7B). Although the function of Kindlin2 in integrin activation is well recognized, the dissection of its integrin-independent function is still in the preliminary stages. This represents the first report of a role for Kindlin2 in NC specification, which provides an entry point for Kindlin2-based research of NC development. How Kindlin2 mechanistically regulates each step of NC development is an important scientific question that awaits further investigation.

MATERIALS AND METHODS

Morpholinos and DNA constructs

Morpholinos (MOs) were purchased from GeneTools and had the following sequences: MO1, 5′-TCACGTCACTGCTTCTCAATCTGGT-3′; MO2, 5′-ATACCATCCAAAGCCATGATTCCT T-3′. The following plasmids were used as templates for the synthesis of mRNAs: pCS2^{+}-xlkindlin2 and pCS2^{+}-xlkindlin2-3′-6Myc, subcloned from pCMV-Sport6-xlkindlin2 (Source BioScience, #IRBHp990C0933D); pCS2^{+}-xlkindlin2-QW/AA and pCS2^{+}-xlkindlin2-QW/AA-3′-6Myc, generated using PCR-based site-directed mutagenesis (Laible and Boonrod, 2009); and pCS2^{+}-hsFGFR1-3′-2FLAG subcloned from pWZL-hsFGFR1-Flag (Addgene, #20486). The plasmid pCS2-mkindlin2-L675E was constructed by PCR, using mkindlin2-L675E-GFP as a template (Li et al., 2017). All of the above constructed plasmids were confirmed by sequencing.

Embryo manipulation

X. laevis and *X. tropicalis* juveniles or adult frogs were purchased from Nasco. The use of frogs for this study was approved by the Ethics Committee of The Chinese University of Hong Kong and licensed by the Department of Health, Hong Kong. Embryos were obtained by *in vitro* fertilization or natural mating, according to the published protocols (Sive et al., 2000) and staged according to Nieuwkoop and Faber (1975). Microinjection was performed bilaterally at stage 2 for western blotting and animal cap assays, or unilaterally at stage 3 for whole-mount *in situ* hybridization and Alcian Blue staining. Animal caps were dissected at stage 9 using forceps, and were cultured in L-15 medium [67% L-15, 7.5 mM Tris-HCl (pH 7.5), 1 mg/ml bovine serum albumin] (Zhao et al., 2008) at room temperature for 4 h or in a 16°C incubator until the stages indicated, before collection.

We titrated a series of injection doses (5, 10 and 20 ng/embryo) of each MO to find the most suitable dose for *Xenopus* embryos. This minimized the non-specific effects induced by MO or the effects due to the innate immune response to MO injection in embryos (Eisen and Smith, 2008; Gentsch et al., 2018). For MO1, 10 ng/embryo was selected, as the 5 ng/embryo exhibited only slight effects on the expression of NC markers and the 20 ng/embryo had a high ratio of lethality before neurulation. For MO2, the 20 ng/embryo was selected, because its penetrance was lower than that of MO1.

β-Galactosidase staining, whole-mount *in situ* hybridization and Alcian Blue staining

For β-galactosidase staining, the embryos were fixed at desired stages using HEMFA buffer [0.1 M 4-(2-hydroxyethyl)-1-piperazineethanesulfonic acid (pH 7.4), 2 mM ethylene glycol-bis(β-aminoethyl ether)-*N*,*N*,*N*′,*N*′-tetraacetic acid, 1 mM $MgSO_4$ and 4% formaldehyde] for 1 h at room temperature. Embryos were washed three times with 1× phosphate-buffered saline, and were then stained [40 mg/ml 5-bromo-4-chloro-3-indolyl-β-D-galactopyranoside, 0.5 M $K_3Fe(CN)_6$, 0.5 M $K_4Fe(CN)_6$ and 100 mM $MgCl_2$] until color appeared (Wang et al., 2015). After re-washing and re-fixation, embryos were dehydrated twice with absolute ethanol for 5 min each, and then stored at −20°C in absolute ethanol. Whole-mount *in situ* hybridization was performed as described previously (Wang et al., 2015, 2019). For Alcian Blue staining, *kindlin2* morphants were fixed at approximately stage 46 using HEMFA. After dehydration with absolute ethanol, embryos were stained in Alcian Blue solution (30% acetic acid, 70% ethanol and 20 mg Alcian Blue) for 3 days. After washing with 95% ethanol and clearing in glycerol/KOH, the cranial cartilages were dissected manually with forceps and imaged with a Nikon SMZ1270 stereomicroscope.

Cell culture and transfection

HEK293T and HeLa cells were cultured in Dulbecco's modified Eagle's medium with 10% fetal bovine serum in a culture incubator at 37°C under 5% CO_2 as described by Li et al. (2018). Transfection was preformed using Lipofectamine 2000 (Invitrogen), following the manufacturer's instructions. Cells were collected 24-48 h after transfection, as indicated, for protein or RNA extraction.

Co-IP and western blot

Proteins were extracted from embryos, as outlined in our previous study (Wang et al., 2015). Dynabeads Protein G (Invitrogen, 10004D) were used to capture the antibody-protein complexes. Membrane-protein extraction was performed using the cell-surface protein biotinylation and isolation kit (Thermo Fisher Scientific, A44390). HeLa cells transfected with *FGFR1-Myc* alone or mixed with *kindlin2* were incubated with biotin. Cell lysates were incubated with Neutravidin resin that can capture the biotinylated membrane proteins. After washing, the proteins were eluted by DTT solutions. Lysates from whole embryos, animal caps, cells and immunoprecipitated samples were resolved by sodium dodecyl sulfate–polyacrylamide gel electrophoresis, transferred to polyvinylidene difluoride membranes and analyzed by immunoblotting. The antibodies used in this study are listed in Table S2.

Quantitative PCR (qPCR)

Total RNAs were extracted from animal caps, cells or whole embryos using TRIzol reagent (Invitrogen, #15596-026). cDNA was generated by PrimeScript RT Reagent Kit (TaKaRa, #RR037A). PCRs were performed using cDNA as a template, on either a general PCR machine (animal cap assay) or on an ABI 7900HT Fast Real-Time PCR instrument (ThermoFisher). The primer pairs used in this study are listed in Table S1.

Confocal microscopy

Kindlin2 KO HT1080 cells stably expressing paxillin-mRuby2 were transfected with either wild-type *Xenopus kindlin2-GFP* or *Xenopus kindlin2 QW/AA-GFP* plasmids. Cell images were captured by a Nikon TiE microscope and an Andor iXon DU-897 EMCCD (Andor), as we have described recently (Liu et al., 2021). Confocal microscopy was used to reveal the cellular localization of *Xenopus* Kindlin2 and FGFR1, and was performed using the same method as outlined previously (Shi et al., 2015). HeLa cells were transfected with *kindlin2-FLAG* and *FGFR1-Myc* plasmids. Fluorescent images were captured by a Leica SP8 confocal microscope after immunostaining.

Integrin-activation assay

Integrin-activation assays were performed as previously described (Li et al., 2017). *Xenopus kindlin2-GFP*, *kindlin2-QW/AA-GFP*, *RFP-tagged talin-FERM* or a mixture of *talin-FERM* and individual *Xenopus kindlin2* constructs were transfected into CHO-A5 cells harboring stable expression of αIIbβ3. The transfected cells were incubated with anti-PAC-1 (BD) antibody, and then stained with Alexa Fluor 633-conjugated goat anti-mouse IgM (Invitrogen). After staining, the cells were analyzed using a BD

FACSCanto Flow Cytometer. Integrin activation was represented by the relative median fluorescence intensities after normalization to the basal PAC1-binding in control cells (CHO-A5).

Generation of *kindlin2* mutant *X. tropicalis* frogs

CRISPR/Cas9-mediated mutant *X. tropicalis* was generated, and the T7E1 assay was performed as described previously (Liu et al., 2016).

Statistical analysis

Statistical analysis was performed using either an unpaired two-tailed chi-squared test or an unpaired two-tailed *t*-test. Data represent mean±s.d. or mean±s.e.m., and $P<0.05$ was considered statistically significant (*$P<0.05$, **$P<0.01$; n.s., no significant difference).

Acknowledgements

We thank Prof. Igor Dawid, Eddy De Robertis, Richard M. Harland, Christof Niehrs, Tomas Pieler, Chuanyue Wu, Yonglong Chen and Cong Yu for the reagents used in this paper. We appreciate the technical assistance of Mr. Chi Bun Wong in this study.

Competing interests

The authors declare no competing or financial interests.

Author contributions

Conceptualization: H.W., Y.D., H.Z.; Methodology: H.W., C.W., Q.L., M.W., J.L.; Validation: H.W., C.W.; Formal analysis: H.W., C.W.; Investigation: H.W., C.W., Q.L., Y.Z., M.W., J.L.; Resources: X.Q., D.C., G.L., J.S., Y.-G.Y., Wood Y.C., Wai Y.C., Y.D., H.Z.; Data curation: Y.D., H.Z.; Writing - original draft: H.W.; Writing - review & editing: C.W., X.Q., D.C., G.L., J.S., Y.-G.Y., Wood Yee Chan, Wai Yee Chan, Y.D., H.Z.; Visualization: H.W., C.W.; Supervision: Y.D., H.Z.; Project administration: Y.D., H.Z.; Funding acquisition: J.S., Y.-G.Y., Y.D., H.Z.

Funding

This work was supported by the National Key R&D Program of China (2016YFE0204700 to H.Z.), by the National Key R&D Program of China, Synthetic Biology Research (2019YFA0904500 to H.Z.), by the Research Grants Council of Hong Kong (14167017 and 14112618 to H.Z.), by the International Partnership Program of Chinese Academy of Sciences (152453KYSB20170031 to Y.-G.Y. and H.Z.), by the Guangdong Natural Science Foundation (2017A030313209 to Y.D.), by the Guangdong Provincial Key Laboratory of Cell Microenvironment and Disease Research (2017B030301018 to Y.D.) and by the Key Research and Development Program of Ningxia Province (2019BEH03003 to J.S.).

Peer review history

The peer review history is available online at https://journals.biologists.com/dev/article-lookup/doi/10.1242/dev.199411

References

Ariizumi, T., Takahashi, S., Chan, T.-C., Ito, Y., Michiue, T. and Asashima, M. (2009). Isolation and differentiation of xenopus animal cap cells. *Curr. Protoc. Stem Cell Biol.* **9**, 1D.5.1-1D.5.31. doi:10.1002/9780470151808.sc01d05s9

Arnaout, M. A., Mahalingam, B. and Xiong, J.-P. (2005). Integrin structure, allostery, and bidirectional signaling. *Annu. Rev. Cell Dev. Biol.* **21**, 381-410. doi:10.1146/annurev.cellbio.21.090704.151217

Avraamides, C. J., Garmy-Susini, B. and Varner, J. A. (2008). Integrins in angiogenesis and lymphangiogenesis. *Nat. Rev. Cancer* **8**, 604-617. doi:10.1038/nrc2353

Baggiolini, A., Varum, S., Mateos, J. M., Bettosini, D., John, N., Bonalli, M., Ziegler, U., Dimou, L., Clevers, H., Furrer, R. et al. (2015). Premigratory and migratory neural crest cells are multipotent in vivo. *Cell Stem Cell* **16**, 314-322. doi:10.1016/j.stem.2015.02.017

Barriga, E. H., Trainor, P. A., Bronner, M. and Mayor, R. (2015). Animal models for studying neural crest development: is the mouse different? *Development* **142**, 1555-1560. doi:10.1242/dev.121590

Bledzka, K., Liu, J., Xu, Z., Perera, H. D., Yadav, S. P., Bialkowska, K., Qin, J., Ma, Y.-Q. and Plow, E. F. (2012). Spatial coordination of kindlin-2 with talin head domain in interaction with integrin β cytoplasmic tails. *J. Biol. Chem.* **287**, 24585-24594. doi:10.1074/jbc.M111.336743

Brewer, J. R., Mazot, P. and Soriano, P. (2016). Genetic insights into the mechanisms of Fgf signaling. *Genes Dev.* **30**, 751-771. doi:10.1101/gad.277137.115

Bronner-Fraser, M. (1986). An antibody to a receptor for fibronectin and laminin perturbs cranial neural crest development in vivo. *Dev. Biol.* **117**, 528-536. doi:10.1016/0012-1606(86)90320-9

Burgar, H. R., Burns, H. D., Elsden, J. L., Lalioti, M. D. and Heath, J. K. (2002). Association of the signaling adaptor FRS2 with fibroblast growth factor receptor 1 (Fgfr1) is mediated by alternative splicing of the juxtamembrane domain. *J. Biol. Chem.* **277**, 4018-4023. doi:10.1074/jbc.M107785200

Canning, C. A., Chan, J. S. K., Common, J. E. A., Lane, E. B. and Jones, C. M. (2011). Developmental expression of the fermitin/kindlin gene family in Xenopus laevis embryos. *Dev. Dyn.* **240**, 1958-1963. doi:10.1002/dvdy.22683

Cheong, S.-M., Choi, S.-C. and Han, J.-K. (2006). Xenopus Dab2 is required for embryonic angiogenesis. *BMC Dev. Biol.* **6**, 63. doi:10.1186/1471-213X-6-63

Chishti, A. H., Kim, A. C., Marfatia, S. M., Lutchman, M., Hanspal, M., Jindal, H., Liu, S.-C., Low, P. S., Rouleau, G. A., Mohandas, N. et al. (1998). The FERM domain: a unique module involved in the linkage of cytoplasmic proteins to the membrane. *Trends Biochem. Sci.* **23**, 281-282. doi:10.1016/S0968-0004(98)01237-7

De Pascalis, C. and Etienne-Manneville, S. (2017). Single and collective cell migration: the mechanics of adhesions. *Mol. Biol. Cell* **28**, 1833-1846. doi:10.1091/mbc.e17-03-0134

Dowling, J. J., Gibbs, E., Russell, M., Goldman, D., Minarcik, J., Golden, J. A. and Feldman, E. L. (2008). Kindlin-2 is an essential component of intercalated discs and is required for vertebrate cardiac structure and function. *Circ. Res.* **102**, 423-431. doi:10.1161/CIRCRESAHA.107.161489

Eisen, J. S. and Smith, J. C. (2008). Controlling morpholino experiments: don't stop making antisense. *Development* **135**, 1735. doi:10.1242/dev.001115

El-Brolosy, M. A., Kontarakis, Z., Rossi, A., Kuenne, C., Günther, S., Fukuda, N., Kikhi, K., Boezio, G. L. M., Takacs, C. M., Lai, S.-L. et al. (2019). Genetic compensation triggered by mutant mRNA degradation. *Nature* **568**, 193-197. doi:10.1038/s41586-019-1064-z

Gentsch, G. E., Spruce, T., Monteiro, R. S., Owens, N. D. L., Martin, S. R. and Smith, J. C. (2018). Innate immune response and off-target mis-splicing are common morpholino-induced side effects in Xenopus. *Dev. Cell* **44**, 597-610.e510. doi:10.1016/j.devcel.2018.01.022

Guo, B., Gao, J., Zhan, J. and Zhang, H. (2015). Kindlin-2 interacts with and stabilizes EGFR and is required for EGF-induced breast cancer cell migration. *Cancer Lett.* **361**, 271-281. doi:10.1016/j.canlet.2015.03.011

Hamidi, H. and Ivaska, J. (2018). Every step of the way: integrins in cancer progression and metastasis. *Nature reviews Cancer* **18**, 533-548. doi:10.1038/s41568-018-0038-z

Harburger, D. S., Bouaouina, M. and Calderwood, D. A. (2009). Kindlin-1 and –2 directly bind the C-terminal region of β integrin cytoplasmic tails and exert integrin-specific activation effects. *J. Biol. Chem.* **284**, 11485-11497. doi:10.1074/jbc.M809233200

Haugsten, E. M., Małecki, J., Bjørklund, S. M. S., Olsnes, S. and Wesche, J. (2008). Ubiquitination of fibroblast growth factor receptor 1 is required for its intracellular sorting but not for its endocytosis. *Mol. Biol. Cell* **19**, 3390-3403. doi:10.1091/mbc.e07-12-1219

LaBonne, C. and Bronner-Fraser, M. (1998). Neural crest induction in Xenopus: evidence for a two-signal model. *Development* **125**, 2403-2414.

Laible, M. and Boonrod, K. (2009). Homemade site directed mutagenesis of whole plasmids. *J. Vis. Exp.* **27**, 1135. doi:10.3791/1135

Li, H., Deng, Y., Sun, K., Yang, H., Liu, J., Wang, M., Zhang, Z., Lin, J., Wu, C., Wei, Z. et al. (2017). Structural basis of kindlin-mediated integrin recognition and activation. *Proc. Natl. Acad. Sci. USA* **114**, 9349-9354. doi:10.1073/pnas.1703064114

Li, T., Deng, Y., Shi, Y., Tian, R., Chen, Y., Zou, L., Kazi, J. U., Rönnstrand, L., Feng, B., Chan, S. O. et al. (2018). Bruton's tyrosine kinase potentiates ALK signaling and serves as a potential therapeutic target of neuroblastoma. *Oncogene* **37**, 6180-6194. doi:10.1038/s41388-018-0397-7

Lignell, A., Kerosuo, L., Streichan, S. J., Cai, L. and Bronner, M. E. (2017). Identification of a neural crest stem cell niche by Spatial Genomic Analysis. *Nat. Commun.* **8**, 1830. doi:10.1038/s41467-017-01561-w

Liu, Z., Cheng, T. T. K., Shi, Z., Liu, Z., Lei, Y., Wang, C., Shi, W., Chen, X., Qi, X., Cai, D. et al. (2016). Efficient genome editing of genes involved in neural crest development using the CRISPR/Cas9 system in Xenopus embryos. *Cell Biosci.* **6**, 22. doi:10.1186/s13578-016-0088-4

Liu, J., Liu, Z., Chen, K., Chen, W., Fang, X., Li, M., Zhou, X., Ding, N., Lei, H., Guo, C. et al. (2021). Kindlin-2 promotes rear focal adhesion disassembly and directional persistence during cell migration. *J. Cell Sci.* **134**, jcs244616. doi:10.1242/jcs.244616

Ma, Z., Zhu, P., Shi, H., Guo, L., Zhang, Q., Chen, Y., Chen, S., Zhang, Z., Peng, J. and Chen, J. (2019). PTC-bearing mRNA elicits a genetic compensation response via Upf3a and COMPASS components. *Nature* **568**, 259-263. doi:10.1038/s41586-019-1057-y

Maharana, S. K. and Schlosser, G. (2018). A gene regulatory network underlying the formation of pre-placodal ectoderm in Xenopus laevis. *BMC Biol.* **16**, 79. doi:10.1186/s12915-018-0540-5

Mayor, R. and Theveneau, E. (2013). The neural crest. *Development* **140**, 2247-2251. doi:10.1242/dev.091751

Mayor, R., Morgan, R. and Sargent, M. G. (1995). Induction of the prospective neural crest of Xenopus. *Development* **121**, 767-777.

Mayor, R., Guerrero, N. and Martinez, C. (1997). Role of FGF and noggin in neural crest induction. *Dev. Biol.* **189**, 1-12. doi:10.1006/dbio.1997.8634

Monsoro-Burq, A.-H., Fletcher, R. B. and Harland, R. M. (2003). Neural crest induction by paraxial mesoderm in *Xenopus* embryos requires FGF signals. *Development* **130**, 3111. doi:10.1242/dev.00531
Montanez, E., Ussar, S., Schifferer, M., Bosl, M., Zent, R., Moser, M. and Fassler, R. (2008). Kindlin-2 controls bidirectional signaling of integrins. *Genes Dev.* **22**, 1325-1330. doi:10.1101/gad.469408
Newbern, J., Zhong, J., Wickramasinghe, R. S., Li, X., Wu, Y., Samuels, I., Cherosky, N., Karlo, J. C., O'Loughlin, B., Wikenheiser, J. et al. (2008). Mouse and human phenotypes indicate a critical conserved role for ERK2 signaling in neural crest development. *Proc. Natl. Acad. Sci. USA* **105**, 17115-17120. doi:10.1073/pnas.0805239105
Nieuwkoop, P. D. and Faber, J. (1975). *Normal Table of Xenopus laevis (Daudin)*. North-Holland
Ornitz, D. M. and Itoh, N. (2015). The Fibroblast Growth Factor signaling pathway. *Wiley Interdiscip. Rev. Dev. Biol.* **4**, 215-266. doi:10.1002/wdev.176
Persaud, A., Alberts, P., Hayes, M., Guettler, S., Clarke, I., Sicheri, F., Dirks, P., Ciruna, B. and Rotin, D. (2011). Nedd4-1 binds and ubiquitylates activated FGFR1 to control its endocytosis and function. *EMBO J.* **30**, 3259-3273. doi:10.1038/emboj.2011.234
Pluskota, E., Dowling, J. J., Gordon, N., Golden, J. A., Szpak, D., West, X. Z., Nestor, C., Ma, Y.-Q., Bialkowska, K., Byzova, T. et al. (2011). The integrin coactivator kindlin-2 plays a critical role in angiogenesis in mice and zebrafish. *Blood* **117**, 4978-4987. doi:10.1182/blood-2010-11-321182
Qi, L., Yu, Y., Chi, X., Xu, W., Lu, D., Song, Y., Zhang, Y. and Zhang, H. (2015). Kindlin-2 interacts with α-actinin-2 and β1 integrin to maintain the integrity of the Z-disc in cardiac muscles. *FEBS Lett.* **589**, 2155-2162. doi:10.1016/j.febslet.2015.06.022
Raabe, E. H., Laudenslager, M., Winter, C., Wasserman, N., Cole, K., LaQuaglia, M., Maris, D. J., Mosse, Y. P. and Maris, J. M. (2008). Prevalence and functional consequence of PHOX2B mutations in neuroblastoma. *Oncogene* **27**, 469-476. doi:10.1038/sj.onc.1210659
Rogalski, T. M., Mullen, G. P., Gilbert, M. M., Williams, B. D. and Moerman, D. G. (2000). The UNC-112 gene in Caenorhabditis elegans encodes a novel component of cell-matrix adhesion structures required for integrin localization in the muscle cell membrane. *J. Cell Biol.* **150**, 253-264. doi:10.1083/jcb.150.1.253
Rognoni, E., Ruppert, R. and Fässler, R. (2016). The kindlin family: functions, signaling properties and implications for human disease. *J. Cell Sci.* **129**, 17-27. doi:10.1242/jcs.161190
Rozario, T., Mead, P. E. and DeSimone, D. W. (2014). Diverse functions of kindlin/fermitin proteins during embryonic development in Xenopus laevis. *Mech. Dev.* **133**, 203-217. doi:10.1016/j.mod.2014.07.004
Sasai, N., Mizuseki, K. and Sasai, Y. (2001). Requirement of FoxD3-class signaling for neural crest determination in Xenopus. *Development* **128**, 2525-2536.
Sauka-Spengler, T. and Bronner-Fraser, M. (2008). A gene regulatory network orchestrates neural crest formation. *Nat. Rev. Mol. Cell Biol.* **9**, 557. doi:10.1038/nrm2428
Shang, N., Lee, J. T. Y., Huang, T., Wang, C., Lee, T. L., Mok, S. C., Zhao, H. and Chan, W. Y. (2020). Disabled-2: a positive regulator of the early differentiation of myoblasts. *Cell Tissue Res.* **381**, 493-508. doi:10.1007/s00441-020-03237-2
Shellard, A. and Mayor, R. (2019). Integrating chemical and mechanical signals in neural crest cell migration. *Curr. Opin. Genet. Dev.* **57**, 16-24. doi:10.1016/j.gde.2019.06.004
Shi, X., Ma, Y.-Q., Tu, Y., Chen, K., Wu, S., Fukuda, K., Qin, J., Plow, E. F. and Wu, C. (2007). The MIG-2/integrin interaction strengthens cell-matrix adhesion and modulates cell motility. *J. Biol. Chem.* **282**, 20455-20466. doi:10.1074/jbc.M611680200
Shi, W., Xu, G., Wang, C., Sperber, S. M., Chen, Y., Zhou, Q., Deng, Y. and Zhao, H. (2015). Heat shock 70-kDa protein 5 (Hspa5) is essential for pronephros formation by mediating retinoic acid signaling. *J. Biol. Chem.* **290**, 577-589. doi:10.1074/jbc.M114.591628
Simões-Costa, M. and Bronner, M. E. (2015). Establishing neural crest identity: a gene regulatory recipe. *Development* **142**, 242-257. doi:10.1242/dev.105445
Simoes-Costa, M. and Bronner, M. E. (2016). Reprogramming of avian neural crest axial identity and cell fate. *Science* **352**, 1570. doi:10.1126/science.aaf2729
Sive, H. L., Grainger, R. M. and Harland, R. M. (2000). *Early Development of Xenopus laevis: A Laboratory Manual*. CSHL Press.
Soldatov, R., Kaucka, M., Kastriti, M. E., Petersen, J., Chontorotzea, T., Englmaier, L., Akkuratova, N., Yang, Y., Häring, M., Dyachuk, V. et al. (2019). Spatiotemporal structure of cell fate decisions in murine neural crest. *Science* **364**, eaas9536. doi:10.1126/science.aas9536
Steventon, B., Araya, C., Linker, C., Kuriyama, S. and Mayor, R. (2009). Differential requirements of BMP and Wnt signalling during gastrulation and neurulation define two steps in neural crest induction. *Development* **136**, 771-779. doi:10.1242/dev.029017
Taylor, K. M. and LaBonne, C. (2007). Modulating the activity of neural crest regulatory factors. *Curr. Opin. Genet. Dev.* **17**, 326-331. doi:10.1016/j.gde.2007.05.012
Testaz, S. and Duband, J.-L. (2001). Central role of the α4β1 integrin in the coordination of avian truncal neural crest cell adhesion, migration, and survival. *Dev. Dyn.* **222**, 127-140. doi:10.1002/dvdy.1181
Wang, C., Chang, J. Y. F., Yang, C., Huang, Y., Liu, J., You, P., McKeehan, W. L., Wang, F. and Li, X. (2013). Type 1 fibroblast growth factor receptor in cranial neural crest cell-derived mesenchyme is required for palatogenesis. *J. Biol. Chem.* **288**, 22174-22183. doi:10.1074/jbc.M113.463620
Wang, C., Kam, R. K. T., Shi, W., Xia, Y., Chen, X., Cao, Y., Sun, J., Du, Y., Lu, G., Chen, Z. et al. (2015). The proto-oncogene transcription factor Ets1 regulates neural crest development through histone deacetylase 1 to mediate output of bone morphogenetic protein signaling. *J. Biol. Chem.* **290**, 21925-21938. doi:10.1074/jbc.M115.644864
Wang, C.-D., Guo, X.-F., Wong, T. C. B., Wang, H., Qi, X.-F., Cai, D.-Q., Deng, Y. and Zhao, H. (2019). Developmental expression of three prmt genes in Xenopus. *Zool. Res.* **40**, 102-107. doi:10.24272/j.issn.2095-8137.2018.064
Wei, X., Xia, Y., Li, F., Tang, Y., Nie, J., Liu, Y., Zhou, Z., Zhang, H. and Hou, F. F. (2013). Kindlin-2 Mediates Activation of TGF-β/Smad Signaling and Renal Fibrosis. *J. Am. Soc. Nephrol.* **24**, 1387-1398. doi:10.1681/ASN.2012101041
Whitman, M. and Melton, D. A. (1992). Involvement of p21ras in Xenopus mesoderm induction. *Nature* **357**, 252-254. doi:10.1038/357252a0
Williams, B. D. and Waterston, R. H. (1994). Genes critical for muscle development and function in Caenorhabditis elegans identified through lethal mutations. *J. Cell Biol.* **124**, 475. doi:10.1083/jcb.124.4.475
Wong, A., Lamothe, B., Lee, A., Schlessinger, J. and Lax, I. (2002). FRS2α attenuates FGF receptor signaling by Grb2- mediated recruitment of the ubiquitin ligase Cbl. *Proc. Natl Acad. Sci. USA* **99**, 6684. doi:10.1073/pnas.052138899
Yu, Y., Wu, J., Wang, Y., Zhao, T., Ma, B., Liu, Y., Fang, W., Zhu, W. G. and Zhang, H. (2012). Kindlin 2 forms a transcriptional complex with β-catenin and TCF4 to enhance Wnt signalling. *EMBO Rep.* **13**, 750-758. doi:10.1038/embor.2012.88
Yu, Y., Wu, J., Guan, L., Qi, L., Tang, Y., Ma, B., Zhan, J., Wang, Y., Fang, W. and Zhang, H. (2013). Kindlin 2 promotes breast cancer invasion via epigenetic silencing of the microRNA200 gene family. *Int. J. Cancer* **133**, 1368-1379. doi:10.1002/ijc.28151
Zhan, J. and Zhang, H. (2018). Kindlins: Roles in development and cancer progression. *Int. J. Biochem. Cell Biol.* **98**, 93-103. doi:10.1016/j.biocel.2018.03.008
Zhang, D., Ighaniyan, S., Stathopoulos, L., Rollo, B., Landman, K., Hutson, J. and Newgreen, D. (2014). The neural crest: a versatile organ system. *Birth Defects Res. C Embryo Today* **102**, 275-298. doi:10.1002/bdrc.21081
Zhao, H., Tanegashima, K., Ro, H. and Dawid, I. B. (2008). Lrig3 regulates neural crest formation in Xenopus by modulating Fgf and Wnt signaling pathways. *Development* **135**, 1283-1293. doi:10.1242/dev.015073

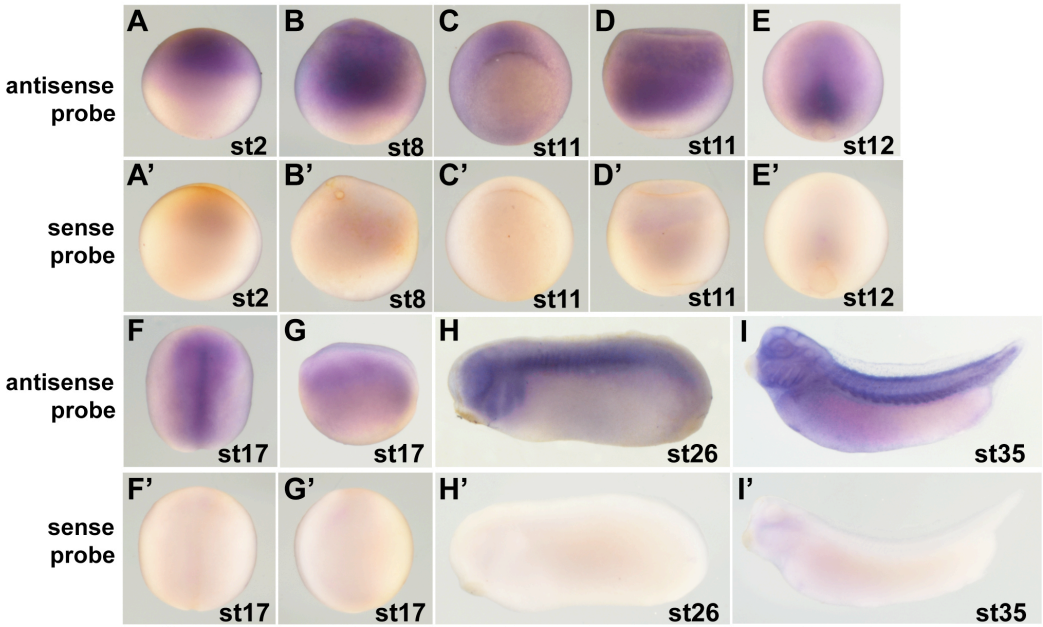

Figure S1. Spatial expression pattern of *kindlin2* in *Xenopus laevis* embryos.

(A-B) *Kindlin2* was expressed in the animal pole during cleavage and blastula stages. (C-E) At the mid-gastrula stage, *kindlin2* was ubiquitously expressed in the whole embryo except for the blastopore (C,D). The signals were then enriched on the dorsal side at later gastrulation (E). (F-G) At the mid-neurula stage, stronger signals appeared in neural plate and adjacent region including the neural crest. (H-I) The expression of *kindlin2* was restricted and maintained in the head, cranial neural crest streams, and somites at tailbud stages. (A'-I') Sense controls, embryos were hybridized with the sense probe of *kindlin2*. A, B, D, A', B' and D', lateral view; C and C', vegetal view; E, F, E' and F', dorsal view; G-I and G'-I', lateral view with head towards left.

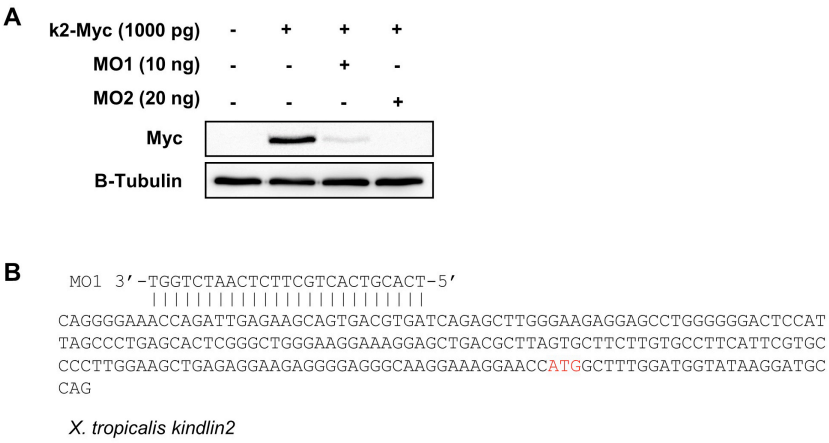

Figure S2. ***Kindlin2*** **MOs attenuate k2-Myc protein translation in embryos**. *X. laevis* embryos were injected with either k2-Myc, k2-Myc+MO1, or k2-Myc+MO2 at two-cell stage. The expression of k2-Myc, kindlin2 with Myc tag at its 3' end, was detected with Western blot using Myc antibody (A). β-Tubulin served as loading control. (B) MO1 can also target *kindlin2* mRNA of *X. tropicalis*.

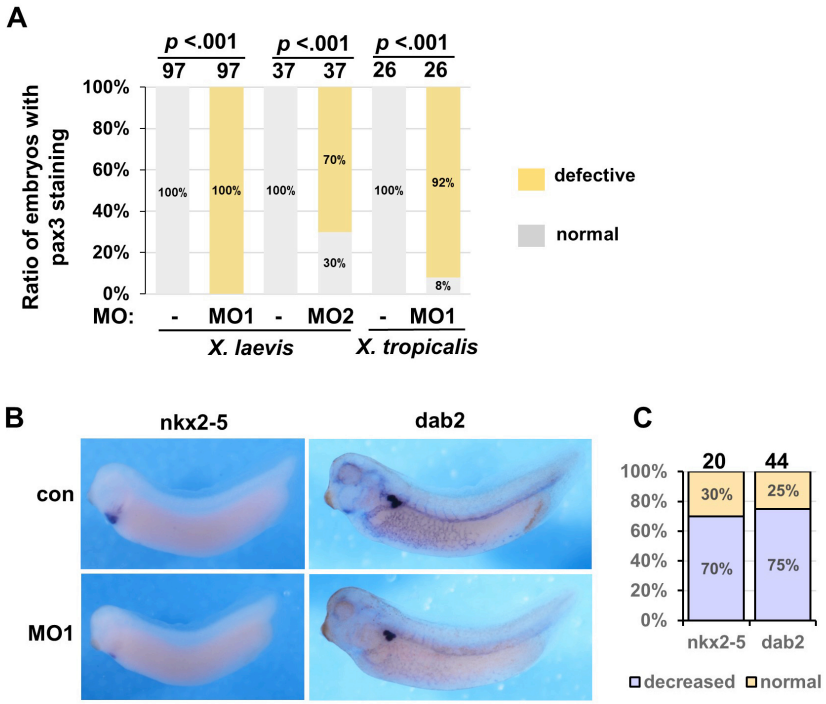

Figure S3. Knockdown of *kindlin2* inhibited expression of *nkx2.5* and *dab2*. (A) Ratio of defective *pax3* expression corresponding to Figure 1F. The total number of embryos analyzed is shown at the top of each column. Chi-square test was employed for statistical analysis. (B-C) Both blastomeres of *X. laevis* embryos at two-cell stage were injected with MO1, and the injected embryos were collected at stage 32 for *nkx2.5* and stage 35 for *dab2* expression examination. Representative images of the whole mount in situ hybridization were shown in (B), and the quantification of the phenotypes was shown in (C).

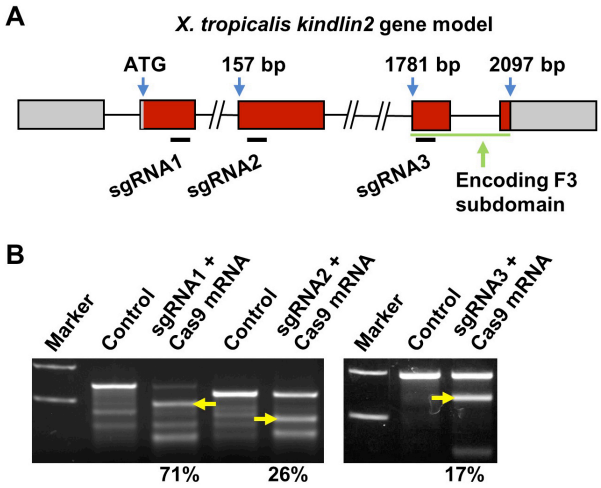

Figure S4. The mutagenic efficiency of three sgRNAs. (A) Illustration of three sgRNA targeting sites. (B) T7E1 enzyme digestion result of embryos bilaterally microinjected with sgRNAs mixed with Cas9 mRNA. The digested bands are indicated by yellow arrows.

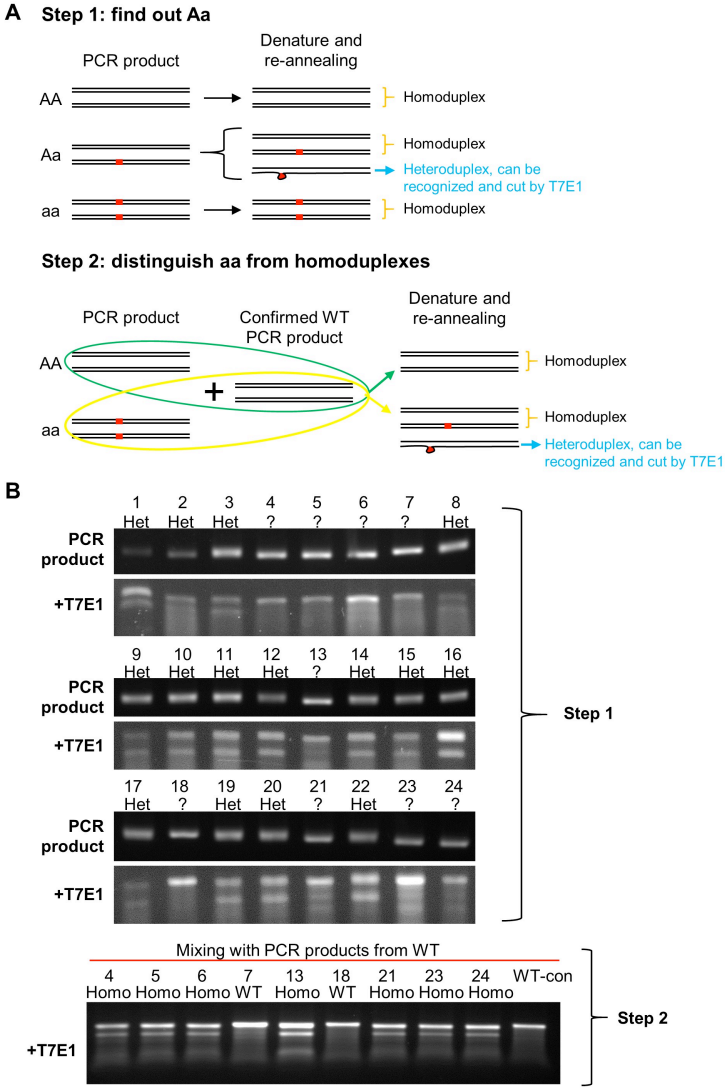

Figure S5. The genotyping result of F2 embryos. (A) Schematic diagram showing the steps for genotyping of individual embryos. (B) Genotyping result of F2 embryos. Het, heterozygotes. Homo, homozygotes. WT-con, PCR product from WT embryos mixed with PCR product from WT embryos. RNAs from No. 6 and No. 13 were used as "k2 $\Delta 10^{-/-}$," to do qPCR in Fig. 2F and 2G.

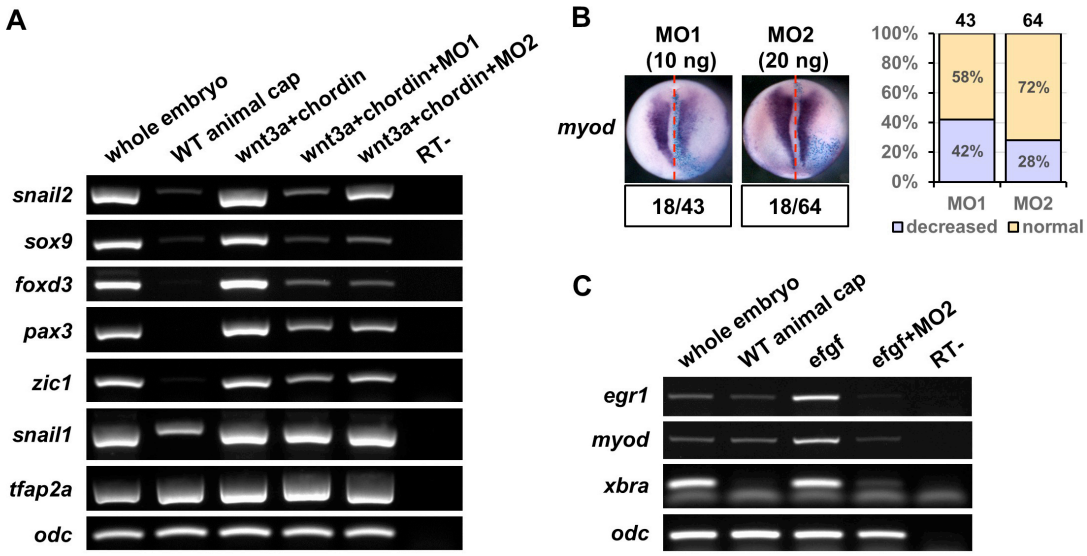

Figure S6. Knockdown of *kindlin2* suppressed the NC induction and FGF signaling in animal cap assay and suppressed the expression of *myod* in *kindlin2* morphants. (A) RT-PCR shows indicated gene expression in the animal caps microinjected with *wnt3a* and *chordin*, or *wnt3a*, *chordin* and MOs. (B) Whole mount *in situ* hybridization showed that the expression of paraxial mesodermal marker gene *myod* was decreased at MO-injected side. (C) The expression of FGF target genes in the animal caps injected with either *efgf,* or the mixture of *efgf* and MO2. *Odc* (ornithine decarboxylase) served as the internal standard control. RT-, control without reverse transcriptase.

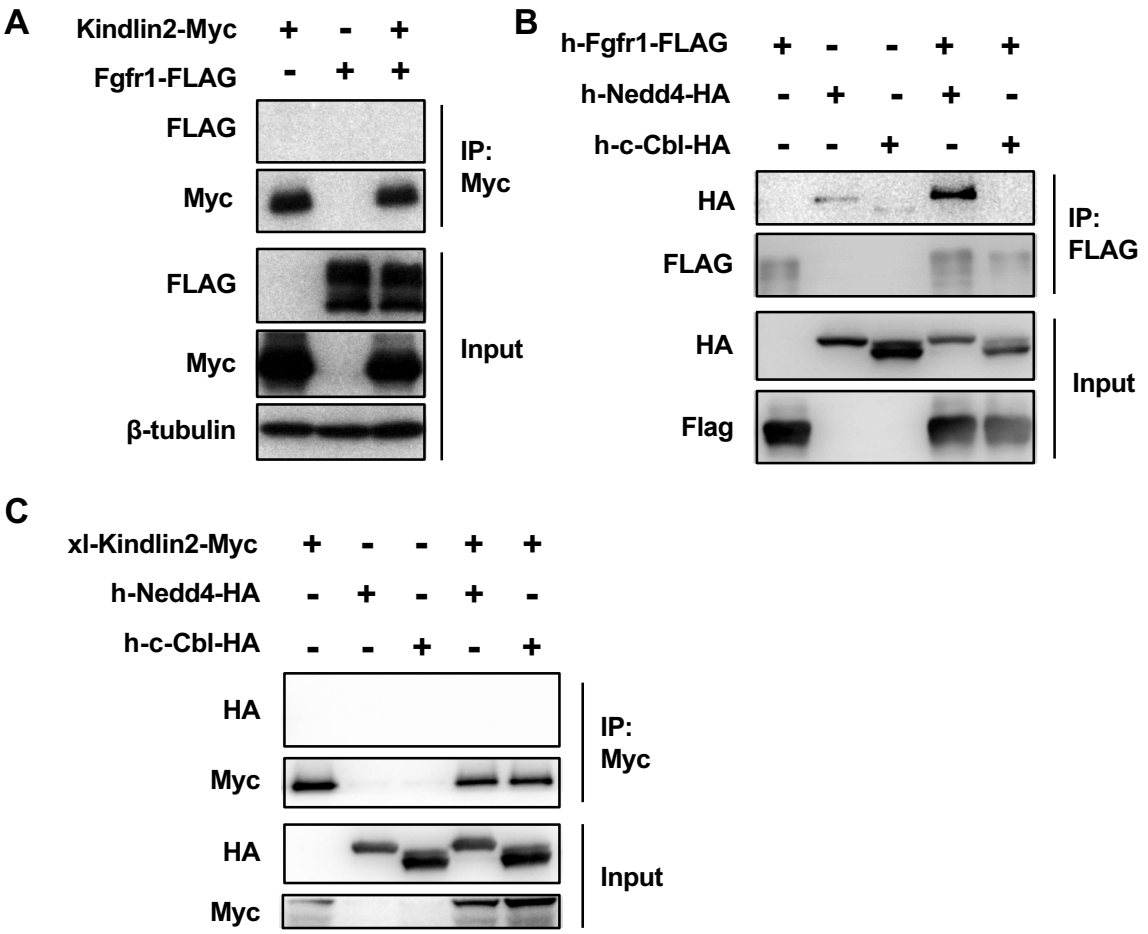

Figure S7. No physical interaction was detected between Kindlin2 and Fgfr1, or Nedd4 or c-Cbl. The possible physical interaction between Kindlin2 and indicated protein was examined by co-immunoprecipitation (Co-IP). (A) Co-IP with protein extracts from embryos microinjected with *kindlin2-Myc* and *Fgfr1-FLAG* alone or in combination. (B, C) Co-IP with protein extracts from HEK293T cells transfected with indicated plasmids.

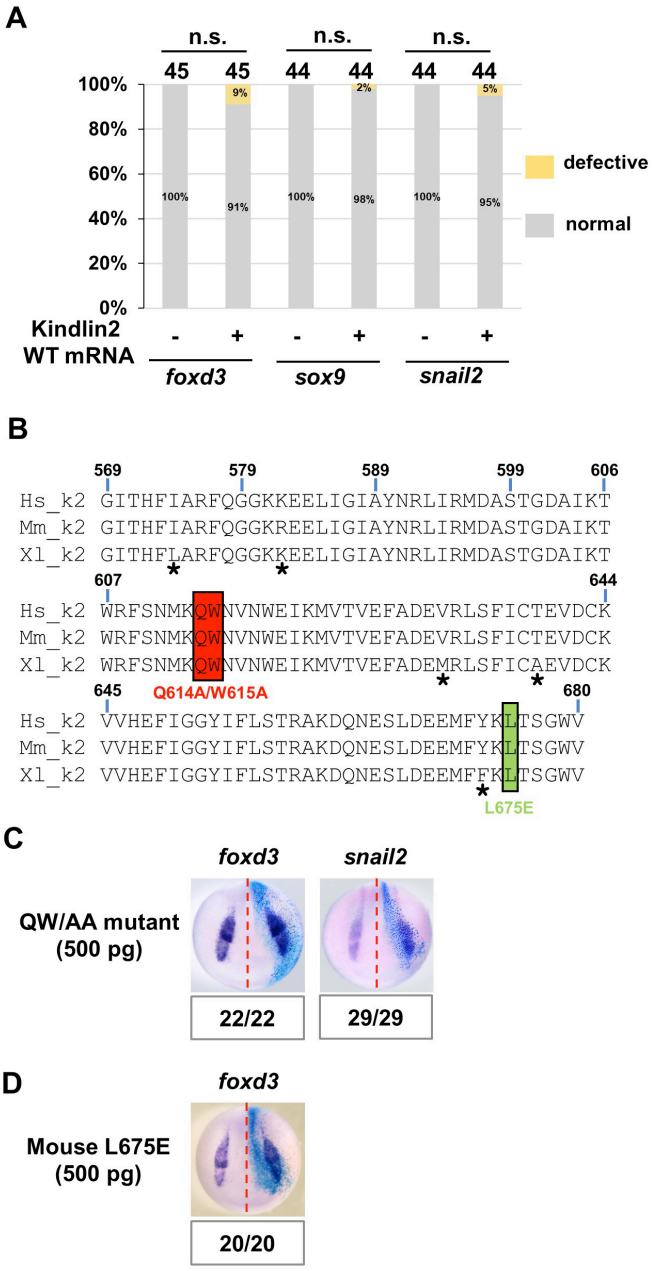

Figure S8. Overexpression of *kindlin2* mutant mRNA has little effect on the expression of NC marker genes. (A) Ratio of defective NC marker genes corresponding to Figure 6A. The total number of embryos analyzed is shown at the top of each column. Chi-square test was employed for statistical analysis. (B) Sequence alignment of Kindlin2 F3 subdomain (residues 569-680). Hs, *Homo sapiens*. Mm, *Mus musculus*. Xl, *Xenopus laevis*. The integrin-binding sites are highlighted in red (residues 614 and 615). The leucine which is essential for the focal adhesion localization of Kindlin2 is highlighted in Kelly green (residue 675). The asterisks indicate the residues that are not conserved among the three species. *Kindlin2 QW/AA*

mRNA (C) or mouse *Kindlin2 L675E* mRNA (D) was injected into one dorsal blastomere of *Xenopus* embryos at four cell stage, and the expression of *foxd3* and *snail2* was examined by whole mount *in situ* hybridization.

Table S1. Primers used for RT-PCR

Click here to download Table S1

Table S2. List of antibodies used in this study

Antibody	Host species	Dilution	Source
FLAG	mouse	1:1000	Sigma, #F1804
Myc	rabbit	1:2500	Cell Signaling Technology, #2278
β tubulin	rabbit	1:2000	Abcam, #ab6064
GAPDH	rabbit	1:1000	Santa Cruz, #sc-25778
ERK	rabbit	1:1000	Millipore, #ABS44
phosphorylated ERK	rabbit	1:1000	Santa Cruz, #sc-16982
FGFR1	rabbit	1:1000	Sigma, #SAB4300488
PAC-1	mouse	1:100	BD, #340535
anti-mouse	sheep	1:5000	GE Healthcare, #NA931
anti-rabbit	goat	1:50000	Abcam, #ab6721